

# WARPED GEOMETRIES OF SEGRE–VERONESE MANIFOLDS\*

SIMON JACOBSSON<sup>†</sup>, LARS SWIJSEN<sup>‡</sup>, JOERI VAN DER VEKEN<sup>§</sup>, AND  
NICK VANNIEUWENHOVEN<sup>¶</sup>

**Abstract.** Segre–Veronese manifolds are smooth manifolds consisting of partially symmetric rank-1 tensors. They are naturally viewed as submanifolds of a Euclidean space of tensors. However, they can also be equipped with other metrics than their induced metrics, such as warped product metrics. We investigate a one-parameter family of warped geometries, which includes the standard Euclidean geometry, and whose parameter controls by how much spherical tangent directions are weighted relative to radial tangent directions. We compute the exponential and logarithmic maps of these warped Segre–Veronese manifolds, including the corresponding starting and connecting geodesics. A closed formula for the intrinsic distance between points on the warped Segre–Veronese manifold is presented. We determine for which warping parameters Segre–Veronese manifolds are geodesically connected and show that they are not geodesically connected in the standard Euclidean geometry. The benefits of connecting geodesics may outweigh using the Euclidean geometry in certain applications. One such application is presented: numerically computing the Riemannian center of mass for averaging rank-1 tensors.

**Key words.** Segre–Veronese manifold; partially symmetric rank-1 tensors; geodesic; exponential map; logarithmic map; warped geometry

**AMS subject classifications.** 15A69; 65F99; 53C22; 53A35; 14N07

**1. Introduction.** The  $k$ th Segre–Veronese manifold  $\mathcal{S}^k$  of partially symmetric rank-1 tensors in the space of  $n_1^{k_1} \times n_2^{k_2} \times \cdots \times n_d^{k_d}$  real arrays is a fundamental set of elementary tensors [55]. Special cases include the punctured plane

$$\mathcal{S}^{(1)} := \mathbb{R}_*^n := \{ \lambda \mathbf{u} \mid \lambda \in \mathbb{R}_{>0}, \|\mathbf{u}\| = 1 \};$$

the manifold of symmetric rank-1 matrices

$$\mathcal{S}^{(2)} := \{ \lambda \mathbf{u} \mathbf{u}^T \mid \lambda \in \mathbb{R}_{>0}, \|\mathbf{u}\| = 1 \} \subset \mathbb{R}^{n \times n},$$

and, more generally, the Veronese manifold  $\mathcal{S}^{(d)}$  of rank-1 symmetric tensors [22, 55]; and the manifold of rank-1 matrices

$$\mathcal{S}^{(1,1)} := \{ \lambda \mathbf{u} \mathbf{v}^T \mid \lambda \in \mathbb{R}_{>0}, \|\mathbf{u}\| = 1, \|\mathbf{v}\| = 1 \} \subset \mathbb{R}^{m \times n},$$

and, more generally, the Segre manifold  $\mathcal{S}^{(1, \dots, 1)}$  of rank-1 tensors [55]. Analogously to the role of rank-1 matrices in a low-rank matrix decomposition, Segre–Veronese manifolds are the basic building blocks of more advanced tensor rank decomposition models [55]. Such sums of partially symmetric rank-1 tensors feature in a plethora of applications in biomedical engineering, chemometrics, computer science, data science, machine learning, psychometrics, signal processing, and statistics, among others; see the overview articles [4, 8, 53, 65, 72, 78] and the references therein.

\***Funding:** This project was funded by BOF project C16/21/002 by the Internal Funds KU Leuven and FWO project G080822N. J. Van der Veken is additionally supported by the Research Foundation—Flanders (FWO) and the Fonds de la Recherche Scientifique (FNRS) under EOS Project G0I2222N.

<sup>†</sup>KU Leuven, Department of Computer Science, Celestijnenlaan 200A – box 2402, B-3000 Leuven, Belgium ([simon.jacobsson@kuleuven.be](mailto:simon.jacobsson@kuleuven.be)). ORCID: 0000-0002-1181-972X

<sup>‡</sup>KU Leuven, Department of Mathematics, Celestijnenlaan 200B – box 2400, B-3000, Leuven, Belgium.

<sup>§</sup>KU Leuven, Department of Mathematics, Celestijnenlaan 200B – box 2400, B-3000, Leuven, Belgium ([joeri.vanderveken@kuleuven.be](mailto:joeri.vanderveken@kuleuven.be)). ORCID: 0000-0003-0521-625X

<sup>¶</sup>KU Leuven, Department of Computer Science, Celestijnenlaan 200A – box 2402, B-3000 Leuven, Belgium ([nick.vannieuwenhoven@kuleuven.be](mailto:nick.vannieuwenhoven@kuleuven.be)); Leuven.AI – KU Leuven Institute for AI, B-3000 Leuven, Belgium. ORCID: 0000-0001-5692-4163

The *algebraic* geometry of the Segre–Veronese manifold and its secant varieties have been thoroughly studied since the 19th century [7]. By contrast, comparatively little is known about the *Riemannian* geometry of Segre–Veronese manifolds, let alone of (the smooth loci of) its higher secant varieties. To our knowledge, only the Euclidean geometry of the Segre manifold of rank-1 tensors (i.e.,  $\mathbf{k} = (1, \dots, 1)$ ) as submanifold of  $\mathbb{R}^{n_1 \times \dots \times n_d}$  was investigated in the prior works [80, 81].

The present paper studies essential properties of the Segre–Veronese manifold  $\mathcal{S}^{\mathbf{k}}$  as a *metric space*. We are primarily interested in characterizing its *geodesics*. These unit-speed curves  $\gamma \subset \mathcal{S}^{\mathbf{k}}$  can informally be thought of as (locally) length-minimizing curves that generalize straight lines in Euclidean spaces. We distinguish between two types: (i) *connecting* geodesics and (ii) *starting* geodesics. First, connecting geodesics, which are related to the manifold’s *logarithmic map*, are characterized by two *endpoints*  $\mathcal{P}, \mathcal{Q} \in \mathcal{S}^{\mathbf{k}}$  and satisfy  $\gamma(0) = \mathcal{P}$  and  $\gamma(\ell) = \mathcal{Q}$ , where  $\ell$  is the distance between  $\mathcal{P}$  and  $\mathcal{Q}$ . Such curves connect  $\mathcal{P}$  and  $\mathcal{Q}$  at the endpoints of  $\gamma$ . Second, starting geodesics, which relate to the manifold’s *exponential map*, are characterized by a point  $\mathcal{P} \in \mathcal{S}^{\mathbf{k}}$  and a tangent vector  $\hat{\mathcal{P}} \in T_{\mathcal{P}}\mathcal{S}^{\mathbf{k}}$  and satisfy  $\gamma(0) = \mathcal{P}$  and  $\gamma'(0) := d\gamma/dt(0) = \hat{\mathcal{P}}$ , i.e., they are curves starting at  $\mathcal{P}$  and emanating in the direction of  $\hat{\mathcal{P}}$ .

**1.1. Applications of geodesics.** Connecting geodesics find application in (i) statistics on manifolds [31], (ii) interpolation on manifolds [86], (iii) approximation of maps into manifolds. First, the definition and computation of statistics of distributions on manifolds often involves connecting geodesics [31]. The simplest statistic, the *Fréchet mean* [32], *Riemannian center of mass*, or *Karcher mean* [48], on a manifold  $\mathcal{M}$  consists of the point(s) that minimize the integral of the squared intrinsic distances to a fixed set of points on  $\mathcal{M}$ . Since the gradient of the distance function from  $x$  to a fixed point  $x^* \in \mathcal{M}$  is the tangent vector at  $x$  of a connecting geodesic between  $x$  and  $x^*$ , connecting geodesics naturally appear in gradient-based Riemannian optimization algorithms for computing such a Fréchet mean [47, 73, 74]. Moreover, connecting geodesics appear in other approximation algorithms for computing the Fréchet mean, such as in [18, 47, 48, 64]. Connecting geodesics also appear in the definition and computation of higher-order statistics on manifolds, such as *principal geodesic analysis* [28, 29, 79]—a generalization of principal component analysis—and the Gaussian distribution and its parameter estimation [17, 73]. They are an essential ingredient in *geodesic regression* [10, 30, 31] and generalizations thereof [41]. Second, many algorithms for interpolation of data on manifolds using, e.g., Bézier curves, splines, and Hermite interpolation, rely on connecting geodesics, for example [33, 46, 62, 68–70, 75, 76, 84, 86–88]. Third, connecting geodesics are an essential building block of algorithms for constructing an approximation of a function from a Euclidean space into a Riemannian manifold. They are used in the Riemannian moving least squares algorithm [35, 36, 77], and the pullback-based methods of [45, 59].

In addition to the aforementioned application areas that use connecting geodesics and which generally also require starting geodesics, the latter have applications in (i) Riemannian optimization [1, 9], and (ii) integration on manifolds [38]. First, starting geodesics (or approximations thereof called *retractions*) are an essential component of *Riemannian optimization algorithms*, which optimize a smooth objective function over a constraint set that is a smooth manifold [1, 9]. Second, starting geodesics, the projection retraction [2], or other retractions are essential in intrinsic integration schemes for vector fields on manifolds, such as the ones arising from differential equations on manifolds (see [23, 38–40, 57, 66, 67]) or the projected ones from dynamic low-rank approximation methods (see [14, 19, 27, 42, 51, 52, 60, 61, 83]).

The foregoing discussion described general potential applications of geodesics. Next, we highlight plausible applications in the context of Segre–Veronese manifolds. Starting geodesics can be used in Riemannian optimization for seeking an approximate *partially symmetric tensor rank decomposition* [7]. Such algorithms were already ap-

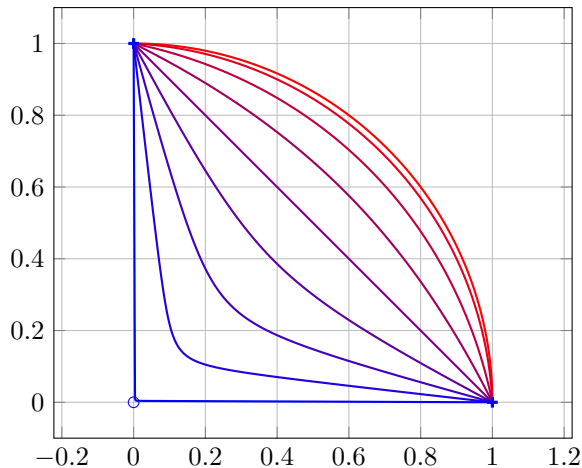


FIGURE 1.1. Geodesics between  $(0, 1)$  and  $(1, 0)$  in the  $\alpha$ -warped geometry for  $\alpha = 0.01$  (the red path approaching the semicircle),  $\frac{1}{4}$ ,  $\frac{1}{2}$ ,  $\frac{3}{4}$ ,  $1$  (the purple straight line),  $\frac{5}{4}$ ,  $\frac{3}{2}$ ,  $\frac{7}{4}$ , and  $1.99$  (the blue path that narrowly avoids the puncture at the origin).

plied to approximate tensor rank decompositions using a retraction in [12] and using geodesics in [81], and to *symmetric tensor rank* or *Waring decompositions* [7, 22] using a retraction in [50]. Connecting geodesics are also natural candidates for designing *recombination operators* in population-based metaheuristic optimization [26] for partially symmetric tensor rank decomposition. Finally, as we will illustrate in section 6, computing a Fréchet mean, which requires connecting and starting geodesics, is a natural alternative to averaging tensor rank decompositions based on factor matrices as was proposed in [15] to improve the robustness of stochastic tensor decompositions.

**1.2. Contributions.** Our main contribution is an analytic expression of the exponential and logarithmic maps of Segre–Veronese manifolds, in Corollary 3.3 and Theorem 4.10 respectively. We also establish a few auxiliary results, such as a neat formula for the distance between points on Segre–Veronese manifolds in Proposition 4.5.

Proposition 4.2 entails that not every pair of partially symmetric rank-1 tensors on a Segre–Veronese manifold can be connected by a minimizing geodesic in the standard Euclidean geometry. In some applications, such as the one presented in section 6, it is more important that any pair of points can be connected by a minimizing geodesic than that Euclidean geometry is used. For this reason, we investigate  $\alpha$ -warped geometries [20] of Segre–Veronese manifolds. These geometries are described in detail in section 2; essentially, they scale, by a factor of  $\alpha > 0$ , the length of all tangent directions which do not infinitesimally change the Euclidean norm. The choice  $\alpha = 1$  corresponds to the usual Euclidean geometry. Figure 1.1 illustrates the minimizing geodesics connecting  $(0, 1)$  and  $(1, 0)$  for various values of  $0 < \alpha < 2$  for the punctured plane  $\mathbb{R}_*^n = \mathcal{S}^{(1)}$ .

**1.3. Outline.** The next section introduces background material from Riemannian geometry and describes  $\alpha$ -warped geometries of  $\mathbb{R}_*^n$ . General  $\alpha$ -warped Segre–Veronese manifolds are obtained as Riemannian embedded submanifolds thereof. We also give an alternative characterization of  $\alpha$ -warped Segre–Veronese manifolds, revealing them to be covered by a warped product of the positive real numbers and a product of spheres, which we call a pre-Segre–Veronese manifold. This characterization is exploited in the subsequent sections: the exponential maps of (pre-)Segre–Veronese manifolds are computed in section 3 and their logarithmic maps are computed in section 4. We present the sectional curvatures of Segre–Veronese manifolds in section 5. Thereafter, in section 6, we detail an example application of connecting

geodesics for computing the Fréchet mean.

**Notation.** For convenience, scalars will be typeset in a lower case, vectors in a bold lower case, tensors in a calligraphic upper case, and manifolds in another calligraphic upper case. We will emphasize that a vector lives in a tangent space by adding an upper dot, e.g.,  $\dot{\mathbf{v}}$ .

Unless otherwise specified,  $(\mathbb{R}^n, \langle \cdot, \cdot \rangle)$  will be abbreviated to  $\mathbb{R}^n$ ; it is the inner product space of  $n$ -dimensional real vectors equipped with the standard Euclidean inner product. If  $\mathcal{M} \subset \mathbb{R}^n$  is any subset, then  $\mathbb{S}(\mathcal{M}) := \{ \mathbf{u} \in \mathcal{M} \mid \|\mathbf{u}\| = 1 \}$  is the space of vectors of  $\mathcal{M}$  of unit Euclidean norm. We use the shorthand  $\mathbb{S}^{n-1} := \mathbb{S}(\mathbb{R}^n)$  for the unit sphere in  $\mathbb{R}^n$ . The angular distance from  $\mathbf{u}$  to  $\mathbf{v}$ , i.e., the arclength of a shortest great circle segment connecting them, is  $\sphericalangle(\mathbf{u}, \mathbf{v}) = \cos^{-1}(\langle \mathbf{v}, \mathbf{u} \rangle) \in [0, \pi]$ .

Let  $\mathcal{M}$  be a manifold. Its tangent space at a point  $x \in \mathcal{M}$  will be denoted by  $T_x\mathcal{M}$ . The exponential map of  $\mathcal{M}$  at  $x$  is  $\exp_x: \Omega_x \rightarrow \mathcal{M}$ , where  $\Omega_x$  is a suitable open neighborhood of  $0 \in T_x\mathcal{M}$ . The logarithmic map of  $\mathcal{M}$  at  $x$  is  $\log_x: \mathcal{M}_x \rightarrow T_x\mathcal{M}$ , where  $\mathcal{M}_x$  is a suitable open neighborhood of  $x \in \mathcal{M}$ . For a curve  $\gamma: \mathbb{R} \rightarrow \mathcal{M}$ , we denote the derivative to its parameter using a prime, i.e.,

$$\gamma'(t) := \frac{d}{dt}\gamma(t).$$

**2.  $\alpha$ -warped geometries for Segre–Veronese manifolds.** The next subsection recalls preliminary results from Riemannian geometry. In particular, the warped product of manifolds will be described. Then, in [subsection 2.2](#), the  $k$ th Segre–Veronese manifold is formally defined and presented as a Riemannian embedded submanifold of a warped geometry of the space of tensors. [Subsection 2.3](#) shows how Segre–Veronese manifolds can be realized as a normal Riemannian covering of a simpler warped product involving only spheres and the nonnegative reals.

**2.1. Warped geometries of  $\mathbb{R}_*^n$ .** Recall that a smooth embedded manifold  $\mathcal{M} \subset \mathbb{R}^N$  equipped with a *Riemannian metric*—an inner product  $g_x: T_x\mathcal{M} \times T_x\mathcal{M} \rightarrow \mathbb{R}$  on its *tangent spaces*  $T_x\mathcal{M}$  that satisfies some technical regularity conditions, see, e.g., [56]—induces an intrinsic metric structure on  $\mathcal{M}$  as follows. A Riemannian metric induces a *Finsler metric*  $\|\dot{\mathbf{x}}\|_x := \sqrt{g_x(\dot{\mathbf{x}}, \dot{\mathbf{x}})}$  for all  $\dot{\mathbf{x}} \in T_x\mathcal{M}$ , which can be used to measure the *length*  $\ell$  of piecewise smooth curves  $\gamma: [0, 1] \rightarrow \mathcal{M}$ :

$$\ell(\gamma) := \int_0^1 \|\gamma'(t)\|_{\gamma(t)} dt.$$

Letting the set of all piecewise smooth curves be our length structure  $L$ , the manifold  $\mathcal{M}$  becomes a *length space* [13]. The *intrinsic metric* induced by this length structure is then defined as

$$\text{dist}_{\mathcal{M}}(x, y) := \inf_{\substack{\gamma \in L, \\ \gamma(0)=x, \gamma(1)=y}} \ell(\gamma).$$

A piecewise smooth curve  $\gamma \in L$  connecting  $x = \gamma(0)$  and  $y = \gamma(1)$  such that the length of  $\gamma$  equals the distance  $\text{dist}_{\mathcal{M}}(x, y)$  is called a *minimizing geodesic* [56]. That is, a minimizing geodesic is a shortest path in  $L$  between  $x$  and  $y$  contained in  $\mathcal{M}$ . More generally, a *geodesic* is any piecewise smooth curve that satisfies the first-order optimality condition, i.e., is a critical point, of the variational problem  $\min_{\gamma \in L} \ell(\gamma)$  subject to appropriate constraints (such as fixing two endpoints). Such curves are always locally length-minimizing [56, Theorem 6.12] in the sense that they are minimizing geodesics on a segment  $\gamma|_{[0,t]}$  for some  $t > 0$ .

The punctured space  $\mathbb{R}_*^n$  is an open submanifold of  $\mathbb{R}^n$ ; hence, it is a smooth manifold. It can be equipped with the standard Euclidean metric  $g$  at  $\mathbf{a} \in \mathbb{R}_*^n$ , so

that  $g_{\mathbf{a}}(\dot{\mathbf{x}}, \dot{\mathbf{y}}) = \langle \dot{\mathbf{x}}, \dot{\mathbf{y}} \rangle = \dot{\mathbf{x}}^T \dot{\mathbf{y}}$ , where  $\dot{\mathbf{x}}, \dot{\mathbf{y}} \in T_{\mathbf{a}}\mathbb{R}_*^n = \mathbb{R}^n$  and  $\langle \cdot, \cdot \rangle$  is the standard Euclidean inner product. This leads to the Euclidean geometry of  $(\mathbb{R}_*^n, g)$ . Other meaningful geometries of  $\mathbb{R}_*^n$  exist. For example,  $\mathbb{R}_*^n$  is diffeomorphic to the product of the positive real line and an  $(n-1)$ -dimensional sphere:  $\mathbb{R}_*^n \simeq \mathbb{R}_{>0} \times \mathbb{S}^{n-1}$ . Under this identification, the above standard Euclidean metric can be expressed as

$$g_{\lambda \mathbf{u}}(\dot{x} \mathbf{u} + \lambda \dot{\mathbf{v}}, \dot{y} \mathbf{u} + \lambda \dot{\mathbf{w}}) = \dot{x} \dot{y} + \lambda^2 \langle \dot{\mathbf{v}}, \dot{\mathbf{w}} \rangle,$$

where  $\dot{x}, \dot{y} \in \mathbb{R} = T_{\lambda} \mathbb{R}_{>0}$  and  $\dot{\mathbf{v}}, \dot{\mathbf{w}} \in \mathbf{u}^{\perp} = T_{\mathbf{u}} \mathbb{S}^{n-1}$ . Herein, the inner products on the right are the inner products inherited from the ambient Euclidean spaces  $\mathbb{R}$  and  $\mathbb{R}^n$ , respectively. Note in particular that the metric that  $\mathbb{R}_*^n$  inherits from  $\mathbb{R}^n$  is *not* equal to the product metric of  $\mathbb{R}_{>0}$  and  $\mathbb{S}^{n-1}$ . Instead, it is a so-called *warped product* [71, Chapter 7] with the identity map as *warping function*. Recall from [71, Chapter 7] that if we are given Riemannian manifolds  $(\mathcal{M}, g)$  and  $(\mathcal{N}, h)$ , then we can construct their warped product with warping function  $f: \mathcal{M} \rightarrow \mathbb{R}$  as  $\mathcal{M} \times_f \mathcal{N} := (\mathcal{M} \times \mathcal{N}, g \times_f h)$ , where

$$(g \times_f h)_{(m,n)}((\dot{\mathbf{m}}_1, \dot{\mathbf{n}}_1), (\dot{\mathbf{m}}_2, \dot{\mathbf{n}}_2)) = g(\dot{\mathbf{m}}_1, \dot{\mathbf{m}}_2) + f^2(m) \cdot h(\dot{\mathbf{n}}_1, \dot{\mathbf{n}}_2).$$

Rather than considering only the Euclidean geometry of  $\mathbb{R}_*^n$ , in this paper, we also consider its  $\alpha$ -warped geometries; that is,

$$(2.1) \quad \mathcal{R}_{\alpha} = (\mathbb{R}_*^n, \zeta^{\alpha}) := \mathbb{R}_{>0} \times_{\alpha \text{Id}} \mathbb{S}^{n-1} \quad \text{with } \alpha > 0,$$

whose warped product metric satisfies

$$(2.2) \quad \zeta_{\lambda \mathbf{u}}^{\alpha}(\dot{x} \mathbf{u} + \lambda \dot{\mathbf{v}}, \dot{y} \mathbf{u} + \lambda \dot{\mathbf{w}}) = \dot{x} \dot{y} + (\alpha \lambda)^2 \langle \dot{\mathbf{v}}, \dot{\mathbf{w}} \rangle.$$

If  $\alpha = 1$ , then the 1-warped geometry is the Euclidean geometry of  $\mathbb{R}_*^n$ , with straight lines as geodesics between points. If  $\alpha > 1$ , then distances in the spherical directions will be elongated, implying that geodesics between points will tend to be forced toward the origin. On the other hand, if  $0 < \alpha < 1$ , then spherical movements are easier, implying that geodesics between points will bend away from the origin. This is visualized in [Figure 1.1](#). The precise form of the geodesics is stated in [Proposition 3.1](#).

**2.2. The  $\alpha$ -warped Segre–Veronese submanifold.** The punctured space  $\mathbb{R}_*^n$  is the most basic example (with  $\mathbf{k} = (1)$ ) of the  $\mathbf{k}$ th Segre–Veronese manifold

$$(2.3) \quad \mathcal{S}_{\pm}^{\mathbf{k}} := \{ \lambda \mathbf{x}_1^{\otimes k_1} \otimes \cdots \otimes \mathbf{x}_d^{\otimes k_d} \mid \lambda \in \mathbb{R}_*, \mathbf{x}_i \in \mathbb{S}^{n_i-1}, i = 1, \dots, d \},$$

where  $\mathbf{x}_i^{\otimes k_i}$  is the  $k_i$ -fold *tensor product* of  $\mathbf{x}_i$  with itself, i.e.,  $\mathbf{x}_i^{\otimes k_i} := \mathbf{x}_i \otimes \cdots \otimes \mathbf{x}_i$ . Recall that the tensor product of vectors in  $\mathbb{R}^{n_j}$ ,  $j = 1, \dots, d$ , can be embedded naturally into the space of  $n_1 \times \cdots \times n_d$  arrays, as follows:

$$(\mathbf{x}_1 \otimes \cdots \otimes \mathbf{x}_d)(i_1, \dots, i_d) := \mathbf{x}_1(i_1) \cdots \mathbf{x}_d(i_d), \quad 1 \leq i_j \leq n_j, j = 1, \dots, d,$$

where  $\mathbf{x}_j \in \mathbb{R}^{n_j}$  and  $\mathbf{x}_j(i_j)$  denotes the  $i_j$ th coefficient of  $\mathbf{x}_j$  with respect to a basis of  $\mathbb{R}^{n_j}$ ; see, e.g., [58]. That is, the coordinates of a tensor product are obtained by multiplying the coordinates of all vectors in all possible ways.

Let us also define the “positive” Segre–Veronese manifold

$$(2.4) \quad \mathcal{S}^{\mathbf{k}} := \{ \lambda \mathbf{u}_1^{\otimes k_1} \otimes \cdots \otimes \mathbf{u}_d^{\otimes k_d} \mid \lambda \in \mathbb{R}_{>0}, \mathbf{u}_i \in \mathbb{S}^{n_i-1}, i = 1, \dots, d \},$$

which is a smooth embedded submanifold that is diffeomorphic to  $\mathbb{R}_{>0} \times \mathbb{S}(\mathcal{S}^{\mathbf{k}})$ . We can thus equip it with the  $\alpha$ -warped metric that it inherits as a submanifold of  $\mathcal{R}_{\alpha} = \mathbb{R}_{>0} \times_{\alpha \text{Id}} \mathbb{S}^{N-1}$  from (2.1), where  $N = n_1^{k_1} \cdots n_d^{k_d}$ . The resulting Riemannian submanifold will be denoted by

$$(2.5) \quad \mathcal{S}_{\alpha}^{\mathbf{k}} := \mathbb{R}_{>0} \times_{\alpha \text{Id}} \mathbb{S}(\mathcal{S}^{\mathbf{k}}) = (\mathcal{S}^{\mathbf{k}}, \zeta^{\alpha}) \subset \mathcal{R}_{\alpha}$$

and we will refer to it as the  $\alpha$ -warped Segre–Veronese manifold.

*Remark 2.1.* If all  $k_i$ 's are even, then  $\mathcal{S}_\pm^{\mathbf{k}}$  consists of two *connected components*, namely the positive Segre–Veronese manifold  $\mathcal{S}^{\mathbf{k}}$  and its mirror image along the origin, namely the “negative” Segre–Veronese manifold  $-\mathcal{S}^{\mathbf{k}}$ . This means that  $p \in \mathcal{S}^{\mathbf{k}}$  and  $q \in -\mathcal{S}^{\mathbf{k}}$  are not connected by any curve in  $\mathcal{S}_\pm^{\mathbf{k}}$ . In particular, there will be no geodesics connecting them. Nevertheless, the two connected components are *isometric*, as  $\varsigma_{(-\lambda)\mathbf{u}}^\alpha = \varsigma_{\lambda\mathbf{u}}^\alpha$  (herein, the metric should be interpreted as being defined on  $\mathbb{R}_{\neq 0}$ ), and we have  $-\mathcal{S}^{\mathbf{k}} = \mathbb{R}_{<0} \times_{\alpha\text{Id}} \mathbb{S}^{N-1}$ . As these two connected components are isometric manifolds, their geometry is the same.

On the other hand, if at least one of the  $k_i$ 's is odd, then it is easy to show that  $\mathcal{S}_\pm^{\mathbf{k}} = \mathcal{S}^{\mathbf{k}} = -\mathcal{S}^{\mathbf{k}}$ . That is, the “regular”, “positive”, and “negative” flavors of the Segre–Veronese manifold all coincide.

Therefore, we will henceforth study the component  $\mathcal{S}^{\mathbf{k}}$  without loss of generality.

**2.3. The  $\alpha$ -warped pre-Segre–Veronese manifold.** We study the geometry of  $\mathcal{S}_\alpha^{\mathbf{k}}$  through the lens of the tensor product  $\otimes$ . By definition,  $\mathcal{S}^{\mathbf{k}}$  is the image of

$$\begin{aligned} \otimes : \mathbb{R}_{>0} \times \mathbb{S}^{n_1-1} \times \cdots \times \mathbb{S}^{n_d-1} &\longrightarrow \mathbb{R}_*^{n_1^{k_1} \times \cdots \times n_d^{k_d}}, \\ (\lambda, \mathbf{u}_1, \dots, \mathbf{u}_d) &\longmapsto \lambda \mathbf{u}_1^{\otimes k_1} \otimes \cdots \otimes \mathbf{u}_d^{\otimes k_d}. \end{aligned}$$

As the domain is a product manifold, its tangent space at  $(\lambda, \mathbf{u}_1, \dots, \mathbf{u}_d)$  is

$$T_\lambda \mathbb{R}_{>0} \times T_{\mathbf{u}_1} \mathbb{S}^{n_1-1} \times \cdots \times T_{\mathbf{u}_d} \mathbb{S}^{n_d-1} = \mathbb{R} \times \mathbf{u}_1^\perp \times \cdots \times \mathbf{u}_d^\perp.$$

We can equip it with the  $\alpha$ -warped product metric

$$(2.6) \quad g_{(\lambda, \mathbf{u}_1, \dots, \mathbf{u}_d)}((\dot{x}, \dot{\mathbf{u}}_1, \dots, \dot{\mathbf{u}}_d), (\dot{y}, \dot{\mathbf{v}}_1, \dots, \dot{\mathbf{v}}_d)) := \dot{x}\dot{y} + (\alpha\lambda)^2 \sum_{i=1}^d k_i \langle \dot{\mathbf{u}}_i, \dot{\mathbf{v}}_i \rangle.$$

The resulting Riemannian manifold will be called the  *$\alpha$ -warped pre-Segre–Veronese manifold*, and it will be denoted by

$$(2.7) \quad \mathcal{P}_\alpha^{\mathbf{k}} = (\mathbb{R}_{>0}, \langle \cdot, \cdot \rangle) \times_{\alpha\text{Id}} \underbrace{((\mathbb{S}^{n_1-1}, k_1 \langle \cdot, \cdot \rangle) \times \cdots \times (\mathbb{S}^{n_d-1}, k_d \langle \cdot, \cdot \rangle))}_{\mathbb{S}^{\mathbf{n}, \mathbf{k}}}.$$

Note that the standard Euclidean inner product on the  $i$ th sphere is weighted by a factor  $k_i$ . The geometry of such a sphere  $(\mathbb{S}^{n_i-1}, k_i \langle \cdot, \cdot \rangle)$  is equivalent to the usual Euclidean geometry of the sphere  $(\mathbb{S}^{\frac{n_i-1}{\sqrt{k_i}}}, \langle \cdot, \cdot \rangle)$  of radius  $\sqrt{k_i}$ .

The key result is that the tensor product takes the pre-Segre–Veronese manifold  $\mathcal{P}_\alpha^{\mathbf{k}}$  in a nice way to the Segre–Veronese manifold  $\mathcal{S}_\alpha^{\mathbf{k}}$ . Specifically, it is a *normal Riemannian covering map* [71], which means that it is a smooth, local isometry in which each point  $\mathcal{T}$  of  $\mathcal{S}_\alpha^{\mathbf{k}}$  has a neighborhood that is *evenly covered* by  $\otimes$ , i.e., the number of elements in the preimage  $\otimes^{-1}(\mathcal{T})$  is constant on  $\mathcal{S}_\alpha^{\mathbf{k}}$ .

LEMMA 2.2. *The map*

$$\otimes : \mathcal{P}_\alpha^{\mathbf{k}} \rightarrow \mathcal{S}_\alpha^{\mathbf{k}}, \quad (\lambda, \mathbf{u}_1, \dots, \mathbf{u}_d) \mapsto \lambda \mathbf{u}_1^{\otimes k_1} \otimes \cdots \otimes \mathbf{u}_d^{\otimes k_d}$$

*is a normal Riemannian covering where the isometric deck transforms are of the form  $\iota_\sigma(\lambda, \mathbf{u}_1, \dots, \mathbf{u}_d) = (\lambda, \sigma_1 \mathbf{u}_1, \dots, \sigma_d \mathbf{u}_d)$  with  $\sigma_i \in \{-1, 1\}$  and  $\sigma_1^{k_1} \cdots \sigma_d^{k_d} = 1$ .*

An elementary but crucial fact about normal Riemannian coverings concerns the lengths of curves in the covered manifold. The next result enables the computation of geodesics in  $\mathcal{S}_\alpha^{\mathbf{k}}$  by studying the geodesics of the warped product  $\mathcal{P}_\alpha^{\mathbf{k}}$ .

LEMMA 2.3. *Let  $\phi : \mathcal{M} \rightarrow \mathcal{N}$  be a normal Riemannian covering. Let  $\gamma \subset \mathcal{N}$  be a smooth curve. Let  $p \in \mathcal{M}$  be any point such that  $\phi(p) = \gamma(0)$ . Then, there exists a unique smooth lift  $\tilde{\gamma} \subset \mathcal{M}$  with  $\tilde{\gamma}(0) = p$  and  $\phi(\tilde{\gamma}) = \gamma$  such that  $\ell(\gamma) = \ell(\tilde{\gamma})$ .*

*In particular, a minimizing geodesic segment  $\gamma \subset \mathcal{N}$  lifts to a minimizing geodesic segment on  $\mathcal{M}$ .*

These lemmas are proved in [Appendix A](#).

**3. The exponential map.** Before presenting the main original contribution in section 4, we briefly investigate the exponential map on the (pre-)Segre–Veronese manifold. The following result is a straightforward generalization of [81, Theorem 1] and its proof, which dealt only with the usual Euclidean geometry (i.e.,  $\alpha = 1$ ) of the Segre manifold (i.e.,  $\mathbf{k} = (1, \dots, 1)$ ). As we will rely on the general strategy of the proof, it is included for self-containedness.

PROPOSITION 3.1 (Starting geodesics of  $\mathcal{P}_\alpha^{\mathbf{k}}$ ). *The unit-speed geodesic  $\gamma$  of the pre-Segre–Veronese manifold  $\mathcal{P}_\alpha^{\mathbf{k}}$  with parameters  $\mathbf{k} \geq 1$  through the point*

$$p = \gamma(0) = (\lambda, \mathbf{u}_1, \dots, \mathbf{u}_d) \in \mathcal{P}_\alpha^{\mathbf{k}}$$

*in the direction of the unit-norm tangent vector*

$$\dot{p} = \gamma'(0) = (\dot{\lambda}, \dot{\mathbf{u}}_1, \dots, \dot{\mathbf{u}}_d) \in \mathbb{T}_p \mathcal{P}_\alpha^{\mathbf{k}}$$

*is given for  $t \in \mathbb{R}$  by  $\gamma_{\dot{p}}(t) = (\lambda(t), \mathbf{u}_1(t), \dots, \mathbf{u}_d(t))$ , where*

$$\begin{aligned} \lambda(t) &= \sqrt{t^2 + 2\lambda\dot{\lambda}t + \lambda^2}, \\ \mathbf{u}_i(t) &= \mathbf{u}_i \cos\left(\frac{\|\dot{\mathbf{u}}_i\|}{\alpha M} g(t)\right) + \frac{\dot{\mathbf{u}}_i}{\|\dot{\mathbf{u}}_i\|} \sin\left(\frac{\|\dot{\mathbf{u}}_i\|}{\alpha M} g(t)\right), \quad i = 1, \dots, d, \\ g(t) &= \tan^{-1}\left(\frac{\sqrt{P^2 + 1}}{\lambda} t + P\right) - \tan^{-1}(P), \end{aligned}$$

*and the constants are  $P = \frac{\dot{\lambda}}{\alpha\lambda M}$  and  $M = \sqrt{\sum_{i=1}^d k_i \|\dot{\mathbf{u}}_i\|^2}$ , provided that  $M > 0$ . Otherwise, if  $M = 0$ , the geodesics are given for all  $-\lambda < \dot{\lambda}t$  by straight lines:*

$$\gamma_{\dot{p}}(t) = (\lambda + \dot{\lambda}t, \mathbf{u}_1, \dots, \mathbf{u}_d).$$

*Proof.* If  $M = 0$ , the proof proceeds exactly as in [81, Proof of Theorem 1]. So we only need to consider the case  $M > 0$ .

Let  $\gamma(t) = (\lambda(t), \mathbf{u}_1(t), \dots, \mathbf{u}_d(t))$  be the geodesic in  $\mathcal{P}_\alpha^{\mathbf{k}}$  from (2.7) with starting conditions  $\gamma(0) = p$  and  $\gamma'(0) = \dot{p}$ . We apply the change of variable  $t \mapsto t(s)$  with  $t(0) = 0$  and  $t'(0) > 0$  such that

$$(3.1) \quad \sigma(s) = (\mu(s), \mathbf{v}_1(s), \dots, \mathbf{v}_d(s)), \text{ with } \|(\mathbf{v}'_1(s), \dots, \mathbf{v}'_d(s))\|_{(\mathbf{v}_1(s), \dots, \mathbf{v}_d(s))} = 1,$$

i.e.,  $\sigma$  has unit *spherical* speed. Then, it holds that  $\|\mathbf{v}'_i(0)\|_{\mathbf{v}_i(0)} = \sqrt{k_i} \|\dot{\mathbf{u}}_i\| t'(0)$ ,  $i = 1, \dots, d$ . From this we find that  $t'(0) = M^{-1}$  where  $M$  is as in the statement of the proposition. After this re-parametrization,  $(\mathbf{v}_1(s), \dots, \mathbf{v}_d(s))$  is a proper geodesic, since it is an arc-length parametrization of a pre-geodesic. This implies [9, Exercise 5.38] that the projection of this geodesic on each of the spheres results in a geodesic. As geodesics on spheres are known [9, Example 5.36] we conclude that

$$(3.2) \quad \mathbf{v}_i(s) = \mathbf{u}_i \cos\left(\frac{\|\dot{\mathbf{u}}_i\|}{M} s\right) + \frac{\dot{\mathbf{u}}_i}{\|\dot{\mathbf{u}}_i\|} \sin\left(\frac{\|\dot{\mathbf{u}}_i\|}{M} s\right), \quad i = 1, \dots, d.$$

The coefficient  $\mu: \mathbb{R} \rightarrow \mathbb{R}$  is determined by solving the *Euler–Lagrange equations* of the length functional, which in the  $\alpha$ -warped geometry becomes

$$(3.3) \quad D = \int_0^T \sqrt{\langle \sigma'(s), \sigma'(s) \rangle_{\sigma(s)}} ds = \int_0^T \sqrt{\mu'(s)^2 + \alpha^2 \mu(s)^2} ds.$$

This ultimately leads to the differential equation  $\alpha^2 \mu(s)^2 + 2\mu'(s)^2 - \mu(s)\mu''(s) = 0$  whose solution is of the form

$$(3.4) \quad \mu(s) = \frac{A}{\cos(\alpha s + B)}.$$

Solving for the constants  $A$  and  $B$  by exploiting the starting conditions, we arrive at  $A = \lambda \cos(B)$  and  $B = \tan^{-1}(\dot{\lambda}/(\alpha\lambda M))$ . In this way, we obtain the pre-geodesic given by (3.2) and (3.4).

The final step, consists of reparameterizing it to arc length. Let  $t$  be the arc-length parameter, such that  $s(t)$  is zero at  $t = 0$ . The arc-length parameterized path  $\chi(t) := \sigma(s(t))$  has unit speed. We can compute

$$\begin{aligned}
 1 = \|\chi'(t)\| &= |s'(t)| \sqrt{\mu'(s(t))^2 + \alpha^2 \mu(s(t))^2} \\
 &= |s'(t)| \sqrt{\frac{\alpha^2 A^2 \sin^2(\alpha s(t) + B)}{\cos^4(\alpha s(t) + B)} + \frac{\alpha^2 A^2}{\cos^2(\alpha s(t) + B)}} \\
 (3.5) \quad &= |s'(t)| \frac{\alpha A}{\cos^2(\alpha s(t) + B)}.
 \end{aligned}$$

From the last equation we conclude that  $s'(t) \neq 0$  on  $(\alpha^{-1}(-\frac{\pi}{2} - B), \alpha^{-1}(\frac{\pi}{2} - B))$  around 0. Therefore, since  $s$  is continuous,  $s'(t)$  is either positive or negative on the interval. Hence, the solution of (3.5) is determined to be of the form

$$(3.6) \quad s = \sigma \alpha^{-1}(\tan^{-1}(A^{-1}t + P) - B),$$

where  $P$  is a constant and  $\sigma \in \{-1, 1\}$ . By plugging in the initial condition  $s(0) = 0$ , we find that  $\tan^{-1}(P) = B$ , so that  $P = \tan(B) = \frac{\dot{\lambda}}{\alpha\lambda M}$ .

We apply the change of variable in (3.6) to (3.2) and (3.4) to obtain the arc-length parametrized geodesic. We continue by exploiting the observation that  $\cos(B) = \alpha\lambda M$  and  $\sin(B) = \dot{\lambda}$ , because  $\dot{\lambda}^2 + \alpha^2 \lambda^2 M^2 = 1$ . Then, we find

$$\begin{aligned}
 \lambda(t) = \mu(s(t)) &= \lambda \cos(B) \sec(\tan^{-1}(\lambda^{-1} \sec(B)t + \tan(B))) \\
 &= \lambda \cos(B) \sqrt{1 + (\lambda^{-1} \sec(B)t + \tan(B))^2} \\
 &= \sqrt{\lambda^2 \cos^2(B) + (t + \lambda \sin(B))^2}.
 \end{aligned}$$

For the spherical paths, we observe that

$$\frac{s(t)}{M} = \frac{\sigma}{\alpha M} (\tan^{-1}(\lambda^{-1} \sec(B)t + P) - \tan^{-1}(P)).$$

Since  $\cos(B) \geq 0$ , we have  $\sec(B) = \sqrt{\sec^2(B)} = \sqrt{\tan^2(B) + 1} = \sqrt{P^2 + 1}$ . The starting condition  $\mathbf{u}'_i(0) = \dot{\mathbf{u}}_i \neq 0$ , for some  $i$ , can finally be exploited to conclude that  $\sigma = 1$ . This concludes the proof.  $\square$

From this result, it immediately follows that the exponential map is well defined almost everywhere.

**COROLLARY 3.2.** *The domain of the exponential map  $\exp_p$  of  $\mathcal{P}_\alpha^{\mathbf{k}}$  is the whole tangent space  $T_p \mathcal{P}_\alpha^{\mathbf{k}}$ , except for the half-line  $\{(\dot{\lambda}, 0, \dots, 0) \mid \dot{\lambda} \leq -\lambda\}$ .*

Having computed the geodesics on the pre-Segre–Veronese manifold, an application of Lemma 2.3 enables us to push them forward with  $\otimes$  to the Segre–Veronese manifold. In this way, we arrive at the latter’s geodesics and the following characterization of the exponential map of  $\mathcal{S}_\alpha^{\mathbf{k}}$ .

**COROLLARY 3.3** (The exponential map of  $\mathcal{S}_\alpha^{\mathbf{k}}$ ). *Let  $\mathcal{P} \in \mathcal{S}_\alpha^{\mathbf{k}}$  be a rank-1 tensor and let  $p = (\lambda, \mathbf{u}_1, \dots, \mathbf{u}_d) \in \otimes^{-1}(\mathcal{P})$  be any of its representations on  $\mathcal{P}_\alpha^{\mathbf{k}}$ . Let  $\dot{\mathcal{P}} \in T_p \mathcal{S}_\alpha^{\mathbf{k}}$ , which can be expressed uniquely as*

$$\dot{\mathcal{P}} = \dot{\lambda} \mathcal{U} + \lambda \left( \nu_{k_1}(\dot{\mathbf{u}}_1) \otimes \mathbf{u}_2^{k_2} \cdots \otimes \mathbf{u}_d^{k_d} + \cdots + \mathbf{u}_1^{k_1} \otimes \cdots \otimes \mathbf{u}_{d-1}^{k_{d-1}} \otimes \nu_{k_d}(\dot{\mathbf{u}}_d) \right),$$



where

$$(3.7) \quad \mathbf{u} = \mathbf{u}_1^{\otimes k_1} \otimes \cdots \otimes \mathbf{u}_d^{\otimes k_d},$$

$$(3.8) \quad \nu_{k_i}(\dot{\mathbf{u}}_i) = (\dot{\mathbf{u}}_i \otimes \mathbf{u}_i^{\otimes(k-1)}) + \cdots + (\mathbf{u}_i^{\otimes(k-1)} \otimes \dot{\mathbf{u}}_i) \quad \text{for all } \dot{\mathbf{u}}_i \in T_{\mathbf{u}_i} \mathbb{S}^n.$$

Let  $\dot{p} = (\dot{\lambda}, \dot{\mathbf{u}}_1, \dots, \dot{\mathbf{u}}_d) \in T_p \mathcal{P}_\alpha^{\mathbf{k}}$  be the corresponding lifted tangent vector. Then,

$$\exp_p(\dot{P}) = \otimes(\exp_p(\dot{p})),$$

insofar as  $\dot{p}$  is in the domain of  $\exp_p$ .

Another interesting consequence of [Proposition 3.1](#) and [Corollary 3.2](#) is that it entails the next result about the radius of the largest open ball in  $T_p \mathcal{S}_\alpha^{\mathbf{k}}$  for which  $\exp$  is a diffeomorphism, i.e., the local injectivity radius of the Segre–Veronese manifold.

**COROLLARY 3.4** (Injectivity radius). *The local injectivity radius of  $\mathcal{P}_\alpha^{\mathbf{k}} \simeq \mathcal{S}_\alpha^{\mathbf{k}}$  at  $p = (\lambda, \mathbf{u}_1, \dots, \mathbf{u}_d)$  is  $\lambda$ . The (global) injectivity radius of  $\mathcal{P}_\alpha^{\mathbf{k}} \simeq \mathcal{S}_\alpha^{\mathbf{k}}$ , i.e., the infimum of the local injectivity radii over the manifold, is zero.*

Note that the latter claim is also immediate from the fact that  $\mathcal{P}_\alpha^{\mathbf{k}} \simeq \mathcal{S}_\alpha^{\mathbf{k}}$  is not a complete metric space. Indeed, the sequence  $p_n = (n^{-1}, \mathbf{u}_1, \dots, \mathbf{u}_d) \in \mathcal{P}_\alpha^{\mathbf{k}} \simeq \mathcal{S}_\alpha^{\mathbf{k}}$  tends to  $(0, \mathbf{u}_1, \dots, \mathbf{u}_d) \notin \mathcal{P}_\alpha^{\mathbf{k}} \simeq \mathcal{S}_\alpha^{\mathbf{k}}$  as  $n \rightarrow \infty$ .

Finally, we highlight that starting geodesics of the pre-Segre–Veronese manifold  $\mathcal{S}_\alpha^{\mathbf{k}}$  can be computed numerically very efficiently by straightforward implementation of the formulas in [Proposition 3.1](#). The cost is about  $\mathcal{O}(\sum_{i=1}^d n_i)$  operations to compute  $M$  and all  $\mathbf{u}_i(t)$ 's, and a constant number of operations for  $\lambda(t)$  and  $g(t)$ .

The computational advantage and simplicity of using geodesics is clear with respect to the default alternative choice, applicable only to the standard Euclidean geometry (i.e.,  $\alpha = 1$ ), namely computing a quasi-optimal projection [[37](#), Chapter 10] with a truncated higher-order singular value decomposition [[24](#)], exploiting the structure of the tangent vectors, as performed in [[54](#)].<sup>1</sup>

**4. The logarithmic map.** We now compute the logarithmic map of the  $\alpha$ -warped (pre-)Segre–Veronese manifold, significantly extending prior results of one of the authors (L. S.) on the Segre manifold ( $\mathbf{k} = (1, \dots, 1)$ ) with the Euclidean metric ( $\alpha = 1$ ) as part of his PhD thesis [[80](#)].

In the next subsection, we first determine a practical characterization of *when* two points on the pre-Segre–Veronese manifold can be connected with a geodesic. Then, in [subsection 4.2](#), we compute this connecting minimizing geodesic if it exists. Finally, we compute minimizing geodesics on the Segre–Veronese manifold between two rank-1 tensors in [subsection 4.3](#) by appropriately lifting them to the pre-Segre–Veronese manifold. Additionally, an efficient matchmaking algorithm is presented to compute this lift, essentially solving a particular combinatorial problem in linear time.

**4.1. Compatibility.** Our main motivation for considering  $\alpha$ -warped geometries of the Segre–Veronese manifold is the observation in [[80](#), Chapter 6] that not all pairs of points on the Segre manifold are connected by a minimizing geodesic. That is, the Segre manifold is not geodesically connected in the standard Euclidean geometry.

The main result of this subsection, [Proposition 4.2](#), will show that the geodesic connectedness of  $\mathcal{P}_\alpha^{\mathbf{k}}$  can be characterized by the following property.

<sup>1</sup>Since partially symmetric tensors form a subset of general tensors, a quasi-optimal projection to the Segre manifold that happens to result in a partially symmetric tensor will be quasi-optimal for the Segre–Veronese manifold as well. A rank- $(r_1, \dots, r_d)$  (parallel) truncated higher-order singular value decomposition of a partially symmetric tensor will be partially symmetric, provided that the  $r_i$ th and  $(r_i + 1)$ th singular values of the  $i$ th flattening (or matricization) are distinct.

DEFINITION 4.1 ( $\alpha$ -compatibility). Consider two points  $p = (\lambda, \mathbf{u}_1, \dots, \mathbf{u}_d)$  and  $q = (\mu, \mathbf{v}_1, \dots, \mathbf{v}_d)$  in  $\mathcal{P}_\alpha^{\mathbf{k}}$ . Let

$$M(p, q) := \text{dist}_{\mathbb{S}^{\mathbf{n}, \mathbf{k}}}((\mathbf{u}_1, \dots, \mathbf{u}_d), (\mathbf{v}_1, \dots, \mathbf{v}_d)) = \sqrt{\sum_{i=1}^d k_i \cdot \angle^2(\mathbf{u}_i, \mathbf{v}_i)}.$$

Then,  $p$  and  $q$  are called  $\alpha$ -compatible if  $M(p, q) < \alpha^{-1}\pi$ .

The dependency of  $M(p, q)$  on the parameters  $\mathbf{k} \geq 1$  will not be emphasized in the notation, instead being implicit in the fact that  $p, q \in \mathcal{P}_\alpha^{\mathbf{k}}$ .

PROPOSITION 4.2. Two points  $p$  and  $q$  can be connected by a minimizing geodesic in  $\mathcal{P}_\alpha^{\mathbf{k}}$  if and only if  $p$  and  $q$  are  $\alpha$ -compatible.

*Proof.* The case where  $\mathbf{u}_i = \mathbf{v}_i$  for all  $i = 1, \dots, d$  corresponds to the case of straight line geodesics (i.e.,  $M(p, q) = 0$ ) in Proposition 3.1. All such  $p$  and  $q$  can be connected by a straight line and since  $M(p, q) = 0$  they are always  $\alpha$ -compatible. Hence, the claim holds in this special case.

The remainder of the proof treats the case  $M(p, q) > 0$ . Let  $p = (\lambda, \mathbf{u}_1, \dots, \mathbf{u}_d) \in \mathcal{P}_\alpha^{\mathbf{k}}$  and  $q = (\mu, \mathbf{v}_1, \dots, \mathbf{v}_d) \in \mathcal{P}_\alpha^{\mathbf{k}}$ . For brevity, we let  $M = M(p, q)$ . We prove the two directions separately.

*Geodesics  $\implies$  compatibility.* Assume that  $p$  and  $q$  are connected by a minimizing geodesic  $\sigma$ , parameterized to have unit spherical speed as in (3.1). Then, Chen's result [20, Lemma 4.4] implies that the projection of  $\sigma$  to the spherical part  $\mathbb{S}^{\mathbf{n}, \mathbf{k}}$ , as in (2.7), is a minimizing unit-speed geodesic. As  $\mathbb{S}^{\mathbf{n}, \mathbf{k}}$  is a product of spheres, each equipped with a scaled Euclidean inner product, this minimizing geodesic is a product of arc segments of the great circles connecting  $\mathbf{u}_i$  and  $\mathbf{v}_i$ . The distance on  $\mathbb{S}^{\mathbf{n}, \mathbf{k}}$  between  $(\mathbf{u}_1, \dots, \mathbf{u}_d)$  and  $(\mathbf{v}_1, \dots, \mathbf{v}_d)$  thus satisfies  $M^2 = \sum_{i=1}^d k_i \cdot \angle^2(\mathbf{u}_i, \mathbf{v}_i)$ .

As  $\sigma$  is a geodesic, it must be a solution of the Euler–Lagrange equation. The proof of Proposition 3.1 then implies that  $\mu(s)$  is the form as in (3.4), where  $A, B \in \mathbb{R}$  are determined by the conditions  $\mu(0) = \lambda$  and  $\mu(M) = \mu$ . We have  $A = \lambda \cos(B)$ , as in the proof of Proposition 3.1, and

$$\frac{\mu(0)}{\mu(M)} = \frac{\lambda}{\mu} = \frac{\cos(B + \alpha M)}{\cos(B)} = \cos(\alpha M) - \sin(\alpha M) \tan(B).$$

Hence,

$$B = \tan^{-1}\left(\cot(\alpha M) - \frac{\lambda\mu^{-1}}{\sin(\alpha M)}\right),$$

provided that  $\alpha M \neq \pi k$  for  $k \in \mathbb{Z}$ . Since  $\sigma(s)$  exists by assumption, the solution  $\mu(s) > 0$  for all  $0 \leq s \leq M$ . The inverse of the cosine has singularities at  $B + \alpha s = \frac{\pi}{2} + k\pi$  for  $k \in \mathbb{Z}$ , so  $\mu(s)$  cannot pass through them and we must have  $-\frac{\pi}{2} + k\pi < B + \alpha s < \frac{\pi}{2} + k\pi$  for all  $0 \leq s \leq M$ . In particular, the endpoint  $s = 0$  implies that  $-\frac{\pi}{2} + k\pi < B < \frac{\pi}{2} + k\pi$ . Consequently,  $0 < \alpha M < \pi$  because we also have that  $M > 0$  and  $\alpha > 0$ . Hence,  $p$  and  $q$  are strictly  $\alpha$ -compatible.

*Compatibility  $\implies$  geodesics.* As before, consider minimizing geodesics  $\mathbf{v}_i(s)$  connecting  $\mathbf{u}_i$  and  $\mathbf{v}_i$  on the sphere  $(\mathbb{S}^{n_i-1}, k_i(\cdot, \cdot))$  for  $i = 1, \dots, d$ . We can parameterize them so that they have unit spherical speed as in (3.1).

If there exists a geodesic connecting  $p$  and  $q$ , it must be a solution of the Euler–Lagrange equation. Proceeding as above, a solution  $\mu(s)$  exists only if  $\alpha M \neq \pi k$  for  $k \in \mathbb{Z}$ . As  $p$  and  $q$  are  $\alpha$ -compatible,  $0 < \alpha M < \pi$ , so  $\mu(s) \subset \mathbb{R}$  is a valid smooth curve. For  $\mu(s)$  to be a geodesic, however, it must also be contained in  $\mathbb{R}_{>0}$  for all  $0 \leq s \leq M$ .

Since  $-\frac{\pi}{2} < B < \frac{\pi}{2}$ , it follows from  $0 < \alpha M < \pi$  that

$$B + \alpha M = \tan^{-1}\left(\cot(\alpha M) - \frac{\lambda\mu^{-1}}{\sin(\alpha M)}\right) + \alpha M < \tan^{-1}(\cot(\alpha M)) + \alpha M,$$

because the arctangent is a monotonically increasing function and  $\frac{\lambda\mu^{-1}}{\sin(\alpha M)} > 0$  when  $\alpha M \in (0, \pi)$ . Exploiting that  $\cot(\alpha M) = \tan(\frac{\pi}{2} - \alpha M)$ , we get  $-\frac{\pi}{2} < B + \alpha M < \frac{\pi}{2}$  for all  $0 < \alpha M < \pi$ . Consequently,  $\mu(s)$  is smooth curve that is strictly positive for all  $0 \leq s \leq M$  and solves the Euler-Lagrange equation. Hence,  $\sigma(s) = (\mu(s), \mathbf{v}_1(s), \dots, \mathbf{v}_d(s))$  is a geodesic connecting  $p$  and  $q$ . This proves the other direction and concludes the proof.  $\square$

The foregoing result implies that by changing the  $\alpha$ -warped metric of  $\mathbb{R}_{>0} \times \mathbb{S}^{\mathbf{n}, \mathbf{k}}$  we can modify whether two points  $p$  and  $q$  are connected by a minimizing geodesic. Specifically, we have the following result.

**PROPOSITION 4.3.** *The pre-Segre-Veronese manifold  $\mathcal{P}_\alpha^{\mathbf{k}}$  is geodesically connected if and only if  $0 < \alpha < \frac{1}{\sqrt{k_1 + \dots + k_d}}$ .*

*Proof.* Let  $p, q \in \mathcal{P}_\alpha^{\mathbf{k}}$ . Then,  $M^2(p, q) \leq \sum_{i=1}^d k_i \pi^2$ , with equality attained at  $p = (\lambda, \mathbf{u}_1, \dots, \mathbf{u}_d)$  and  $q = (\lambda, -\mathbf{u}_1, \dots, -\mathbf{u}_d)$ . The result follows from [Proposition 4.2](#).  $\square$

**4.2. Pre-Segre-Veronese manifolds.** Having determined when two points on the pre-Segre-Veronese manifold  $\mathcal{P}_\alpha^{\mathbf{k}}$  can be connected by a minimizing geodesic, we proceed by computing such a geodesic between two  $\alpha$ -compatible points.

**THEOREM 4.4** (Connecting geodesics of  $\mathcal{P}_\alpha^{\mathbf{k}}$ ). *Let  $p = (\lambda, \mathbf{u}_1, \dots, \mathbf{u}_d)$  and  $q = (\mu, \mathbf{v}_1, \dots, \mathbf{v}_d)$  be  $\alpha$ -compatible points of  $\mathcal{P}_\alpha^{\mathbf{k}}$ . Let  $M = M(p, q)$  from [Definition 4.1](#) and let  $\mathbf{u}_i^\perp$  be any unit-norm vector orthogonal to  $\mathbf{u}_i$ . Let*

$$\begin{aligned} \dot{\lambda} &= \frac{\lambda\alpha M(\cos(\alpha M) - \lambda\mu^{-1})}{\sin(\alpha M)}, \\ \dot{\mathbf{u}}_i &= \langle (\mathbf{u}_i, \mathbf{v}_i) \rangle \cdot \begin{cases} \frac{(\text{Id} - \mathbf{u}_i \mathbf{u}_i^T) \mathbf{v}_i}{\sin \langle (\mathbf{u}_i, \mathbf{v}_i) \rangle}, & \text{if } \mathbf{v}_i \neq -\mathbf{u}_i, \\ \mathbf{u}_i^\perp, & \text{if } \mathbf{v}_i = -\mathbf{u}_i, \end{cases} \quad i = 1, \dots, d, \end{aligned}$$

if  $M > 0$ , and

$$\dot{\lambda} = \mu - \lambda, \quad \text{and} \quad \dot{\mathbf{u}}_i = 0, \quad i = 1, \dots, d,$$

if  $M = 0$ . Then  $\dot{\mathbf{p}} = (\dot{\lambda}, \dot{\mathbf{u}}_1, \dots, \dot{\mathbf{u}}_d)$  is a tangent vector at  $p$  and

$$\gamma: [0, \text{dist}_{\mathcal{P}_\alpha^{\mathbf{k}}}(p, q)] \longrightarrow \mathcal{P}_\alpha^{\mathbf{k}}, \quad t \longmapsto \exp_p\left(t \frac{\dot{\mathbf{p}}}{\sqrt{\dot{\lambda}^2 + \alpha^2 M^2 \lambda^2}}\right)$$

is a unit-speed minimizing geodesic connecting  $p = \gamma(0)$  and  $q = \gamma(\text{dist}_{\mathcal{P}_\alpha^{\mathbf{k}}}(p, q))$ .

*Proof.* The case  $M = 0$  follows immediately from [Proposition 3.1](#). Hence, in the remainder of the proof we consider the case  $M > 0$ .

The proof of [Proposition 3.1](#) showed that a geodesic, parameterized to have unit speed on the product of spheres, is of the form given in [\(3.1\)](#), [\(3.2\)](#), and [\(3.4\)](#). Chen's result [[20](#), Lemma 4.4] implies that for a minimizing geodesic,  $\mathbf{v}_i(t)$  is a shortest great circle segment on  $\mathbb{S}^{n_i-1}$  with constant speed such that  $\mathbf{v}_i(0) = \mathbf{u}_i$  and  $\mathbf{v}_i(M) = \mathbf{v}_i$ . Consequently, if  $\mathbf{v}_i \neq -\mathbf{u}_i$ , then taking

$$\dot{\mathbf{u}}_i = \log_{\mathbf{u}_i}(\mathbf{v}_i) := \langle (\mathbf{u}_i, \mathbf{v}_i) \rangle \cdot \frac{(\text{Id} - \mathbf{u}_i \mathbf{u}_i^T) \mathbf{v}_i}{\sin \langle (\mathbf{u}_i, \mathbf{v}_i) \rangle},$$

where  $\log$  is the logarithmic map of the unit sphere  $\mathbb{S}^{n_i-1}$  [9, Example 10.21], satisfies the boundary conditions of the geodesic:

$$\begin{aligned}\mathbf{v}_i(0) &= \mathbf{u}_i, \\ \mathbf{v}_i(M) &= \mathbf{u}_i \cos \angle(\mathbf{u}_i, \mathbf{v}_i) + \frac{(\text{Id} - \mathbf{u}_i \mathbf{u}_i^T) \mathbf{v}_i}{\sin \angle(\mathbf{u}_i, \mathbf{v}_i)} \sin \angle(\mathbf{u}_i, \mathbf{v}_i) = \mathbf{v}_i.\end{aligned}$$

Herein, we used that  $\|\dot{\mathbf{u}}_i\| = \angle(\mathbf{u}_i, \mathbf{v}_i)$  as can be verified through standard trigonometric computations. If, on the other hand,  $\mathbf{v}_i = -\mathbf{u}_i$ , then any vector  $\mathbf{u}_i^\perp$  perpendicular to  $\mathbf{u}_i$  and of Euclidean length  $\|\mathbf{u}_i^\perp\| = \angle(\mathbf{u}_i, \mathbf{v}_i) = \pi$  leads to a great circle through  $\mathbf{u}_i$  and  $\mathbf{v}_i$  on  $(\mathbb{S}^{n_i-1}, k_i \langle \cdot, \cdot \rangle)$  such that the distance between them is  $\sqrt{k_i} \pi$ . Note that in both cases, we have  $M^2 = \sum_{i=1}^d k_i \angle(\mathbf{u}_i, \mathbf{v}_i)^2 = \sum_{i=1}^d k_i \|\dot{\mathbf{u}}_i\|^2$ .

The points  $p$  and  $q$  are assumed to be  $\alpha$ -compatible, so that the boundary value problem obtained from the Euler–Lagrange equation of the length functional in (3.3) with  $\mu(0) = \lambda$  and  $\mu(M) = M$  has a unique solution. Since  $\mu = \mu(M) = \lambda \frac{\cos(B)}{\cos(B+\alpha M)}$ , we find

$$\lambda \mu^{-1} = \frac{\cos(B) \cos(\alpha M) - \sin(B) \sin(\alpha M)}{\cos(B)} = \cos(\alpha M) - \sin(\alpha M) \frac{\dot{\lambda}}{\alpha M \lambda},$$

having used  $\tan(B) = P = \frac{\dot{\lambda}}{\alpha M \lambda}$ . Solving for  $\dot{\lambda}$ , we obtain

$$\dot{\lambda} = \frac{\alpha M \lambda}{\sin(\alpha M)} (\cos(\alpha M) - \lambda \mu^{-1}).$$

Since  $\|(\dot{\lambda}, \dot{\mathbf{u}}_1, \dots, \dot{\mathbf{u}}_d)\|^2 = \dot{\lambda}^2 + \alpha^2 \lambda^2 M^2$ , normalizing  $\dot{\mathbf{x}}$  by this quantity yields a unit-norm vector. Then,  $\gamma$  from the statement of the proposition is a minimizing geodesic connecting  $p$  and  $q$ , parameterized by unit speed. As a result,  $q$  is reached at  $t = \text{dist}_{\mathcal{P}_\alpha^{\mathbf{k}}}(p, q)$ .  $\square$

An immediate consequence of the proof of the previous theorem is the following expression for the distance between points on the pre-Segre–Veronese manifold.

**PROPOSITION 4.5** (Distance between compatible points on  $\mathcal{P}_\alpha^{\mathbf{k}}$ ). *Consider two points  $p = (\lambda, \mathbf{u}_1, \dots, \mathbf{u}_d) \in \mathcal{P}_\alpha^{\mathbf{k}}$  and  $q = (\mu, \mathbf{v}_1, \dots, \mathbf{v}_d) \in \mathcal{P}_\alpha^{\mathbf{k}}$  that are  $\alpha$ -compatible. Let  $M := M(p, q)$  from Definition 4.1. Then,*

$$(4.1) \quad \text{dist}_{\mathcal{P}_\alpha^{\mathbf{k}}}(p, q) = \sqrt{\lambda^2 - 2\lambda\mu \cos(\alpha M) + \mu^2}.$$

*Proof.* For  $M(p, q) = 0$ , it follows immediately from Proposition 3.1 that the distance between  $p$  and  $q$  on  $\mathcal{P}_\alpha^{\mathbf{k}}$  is equal to  $|\lambda - \mu|$ . This coincides with (4.1).

Let  $M(p, q) > 0$ . The proof of Theorem 4.4 shows that  $q$  is reached at  $s = M(p, q)$  when the geodesic is parameterized to have unit speed on the spheres. Hence, we can use the reparameterization in (3.6) to determine the distance  $\text{dist}_{\mathcal{P}_\alpha^{\mathbf{k}}}(p, q)$ . It follows that it can be expressed as

$$\text{dist}_{\mathcal{P}_\alpha^{\mathbf{k}}}(p, q) = \lambda \cos(B) (\tan(B + \alpha M) - \tan B),$$

where  $B = \arctan\left(\frac{\cos(\alpha M) - \lambda \mu^{-1}}{\sin(\alpha M)}\right)$ . We proceed by simplifying this formula.

The addition formula for  $\tan$  implies that

$$\begin{aligned}\text{dist}_{\mathcal{P}_\alpha^{\mathbf{k}}}(p, q) &= \lambda \cos(B) \frac{\sin(B) \cos(\alpha M) + \cos(B) \sin(\alpha M)}{\cos(B) \cos(\alpha M) - \sin(B) \sin(\alpha M)} - \lambda \sin(B) \\ &= \frac{\lambda \sin(\alpha M)}{\cos(B) \cos(\alpha M) - \sin(B) \sin(\alpha M)}.\end{aligned}$$

We now substitute for  $B$  and use that  $\cos(\arctan x) = 1/\sqrt{1+x^2}$  and  $\sin(\arctan x) = x/\sqrt{1+x^2}$  to obtain

$$\begin{aligned} \text{dist}_{\mathcal{P}_\alpha^{\mathbf{k}}}(p, q) &= \frac{\lambda \sin(\alpha M) \sqrt{1 + \left(\frac{\cos(\alpha M) - \lambda \mu^{-1}}{\sin(\alpha M)}\right)^2}}{\cos(\alpha M) - \left(\frac{\cos(\alpha M) - \lambda \mu^{-1}}{\sin(\alpha M)}\right) \sin(\alpha M)} \\ &= \frac{\lambda \sqrt{\sin^2(\alpha M) + (\cos(\alpha M) - \lambda \mu^{-1})^2}}{\lambda \mu^{-1}}, \end{aligned}$$

having used that  $0 < \sin(\alpha M)$  because  $0 < \alpha M < \pi$ . The last equation is equivalent to (4.1), concluding the proof.  $\square$

A formula, equivalent to (4.1), is

$$(4.2) \quad \text{dist}_{\mathcal{P}_\alpha^{\mathbf{k}}}(p, q) = \sqrt{(\lambda - \mu)^2 + 4\lambda\mu \sin(\alpha M/2)},$$

which is more numerically stable for points that are close together.

The distance between  $p$  and  $q$  on  $\mathcal{P}_\alpha^{\mathbf{k}}$  is thus given by the *law of cosines* applied to an imaginary triangle where one side has length  $\lambda$ , the other side has length  $\mu$ , and the angle is the spherical distance  $M(p, q)$  multiplied by the warping factor  $\alpha$ . We thus immediately obtain the following result.

**COROLLARY 4.6.** *The distance  $\text{dist}_{\mathcal{P}_\alpha^{\mathbf{k}}}(p, q)$  is monotonically increasing as a function of the spherical distance  $M(p, q)$  for  $0 < \alpha M(p, q) < \pi$ .*

Interestingly, we can also determine the distance between *incompatible* points, even though *minimizing* geodesics do not exist between them. While a minimizing geodesic does not exist, there exists a limiting piecewise smooth curve that is the infimizer of the length functional in (3.3). In Figure 1.1, for example, this limiting piecewise smooth curve is the straight line from  $(1, 0)$  to  $(0, 0)$ , composed with the straight line from  $(0, 0)$  to  $(0, 1)$ .

Before presenting this result, we will need to the following technical lemma to prove it. It states that a geodesic starting at  $\lambda$  whose angular distance is  $\frac{\pi}{2\alpha}$  will have length equal to  $\lambda$ . In fact, the details of the proof reveal that such a geodesic is the straight line segment  $\gamma(t) = (\lambda - t, 0, \dots, 0) \in \mathcal{P}_\alpha^{\mathbf{k}}$  for  $t \in [0, \lambda)$ . The technical lemma is as follows.

**LEMMA 4.7.** *Let  $\alpha > 0$  and  $\lambda > 0$ . We have*

$$(4.3) \quad \inf_{\mu(0)=\lambda} \int_0^{\frac{\pi}{2\alpha}} \sqrt{\mu'(s)^2 + \alpha^2 \mu(s)^2} ds = \lambda,$$

where  $\mu: \mathbb{R} \rightarrow \mathbb{R}_{\geq 0}$  is as in (3.4).

*Proof.* The integral measures the distance between  $p = (\lambda, \mathbf{u}_1, \dots, \mathbf{u}_d) \in \mathcal{P}_\alpha^{\mathbf{k}}$  and  $q = (\mu, \mathbf{v}_1, \dots, \mathbf{v}_d) \in \mathcal{P}_\alpha^{\mathbf{k}}$  subject only to the constraint that  $M(p, q) = \frac{\pi}{2\alpha}$ . Hence, using Proposition 4.5, the optimization problem is equivalent to

$$\inf_{\mu \in \mathbb{R}_{>0}} \sqrt{\lambda^2 - 2\lambda\mu \cos\left(\alpha \frac{\pi}{2\alpha}\right) + \mu^2} = \inf_{\mu \in \mathbb{R}_{>0}} \sqrt{\lambda^2 + \mu^2} = \lambda.$$

This proves the claim.  $\square$

With the foregoing result, we can prove the following claim about the distance between  $\alpha$ -incompatible points.

**PROPOSITION 4.8** (Distance between incompatible points on  $\mathcal{P}_\alpha^{\mathbf{k}}$ ). *Two  $\alpha$ -incompatible points  $p = (\lambda, \mathbf{u}_1, \dots, \mathbf{u}_d) \in \mathcal{P}_\alpha^{\mathbf{k}}$  and  $q = (\mu, \mathbf{v}_1, \dots, \mathbf{v}_d) \in \mathcal{P}_\alpha^{\mathbf{k}}$  are at*

$$\text{dist}_{\mathcal{P}_\alpha^{\mathbf{k}}}(p, q) = \lambda + \mu.$$

*Proof.* We observe again the notation from the proof of [Proposition 3.1](#). In particular, let  $\sigma(s) = (\nu(s), \mathbf{v}_1(s), \dots, \mathbf{v}_d(s))$  be a curve parameterized as in [\(3.1\)](#). Consider the (piecewise) curve  $\nu(s)$  which is obtained as a (generalized) solution of the second-order Euler–Lagrange differential equation with as boundary conditions that  $q$  is reached from  $p$  with angular distance  $M = M(p, q)$ . We claim that the length of this geodesic is  $\lambda + \mu$ .

*Lower bound.* The length of  $\nu$  is

$$\begin{aligned} \ell(\nu) &\geq \int_0^{\frac{\pi}{2\alpha}} \sqrt{\nu'(s)^2 + \alpha^2 \nu^2(s)} \, ds + \int_{M-\frac{\pi}{2\alpha}}^M \sqrt{\nu'(s)^2 + \alpha^2 \nu^2(s)} \, ds \\ &\geq \inf_{\nu_1(0)=\lambda} \int_0^{\frac{\pi}{2\alpha}} \sqrt{\nu_1'(s)^2 + \alpha^2 \nu_1^2(s)} \, ds + \inf_{\nu_2(M)=\mu} \int_{M-\frac{\pi}{2\alpha}}^M \sqrt{\nu_2'(s)^2 + \alpha^2 \nu_2^2(s)} \, ds \\ &= \lambda + \mu. \end{aligned}$$

The correctness of these steps is established as follows. The incompatibility of  $p$  and  $q$  means that  $M \geq \pi\alpha^{-1}$ . Hence, in the first step, we discarded the integration over the middle section of the curve  $\gamma$ . The second step replaced the two remaining segments of  $\nu$  by optimal geodesic segments  $\nu_1$  and  $\nu_2$  that only have one constraint on their endpoints active, while maintaining the correct angular distance. Note in particular that we do not impose that the optimal  $\nu_1$  and  $\nu_2$  curves connect to one another at their free endpoints  $\nu_1(\pi/2\alpha)$  and  $\nu_2(M - \pi/2\alpha)$ —it can be deduced from the proof of [Lemma 4.7](#) that  $\nu_1$  and  $\nu_2$  actually both end up in  $0 \in \overline{\mathbb{R}_{>0}}$ . The final step consists of applying [Lemma 4.7](#) to both summands, exploiting for the second summand that fixing an endpoint is equivalent to fixing a starting point and then integrating backward.

*Upper bound.* Since minimizing geodesics have the shortest length among all piecewise smooth curves connecting  $p$  and  $q$ , we can upper bound  $\ell(\nu)$  by considering any other path  $\pi(s) = (\kappa(s), \mathbf{u}_1(s), \dots, \mathbf{u}_d(s))$ . Specifically, consider the straight line from  $\lambda$  to  $\epsilon$  on  $\mathbb{R}_{>0}$ , then a complete rotation (over angular distance  $M$  on the spheres, while keeping  $\kappa(s)$  constant (i.e.,  $\kappa'(s) = 0$  and  $\kappa(s) = \epsilon$  on this segment), and finally moving from  $\epsilon$  up to  $\mu$  on  $\mathbb{R}_{>0}$ . The length of this path satisfies

$$\begin{aligned} \ell(\nu) &\leq \ell(\pi) = |\lambda - \epsilon| + |\mu - \epsilon| + \int_0^M \sqrt{\kappa'(s)^2 + \alpha^2 \kappa^2(s)} \, ds \\ &= \lambda + \mu - 2\epsilon + \alpha M \epsilon. \end{aligned}$$

Because of the incompatibility, we have  $\alpha M - 2 \geq \pi - 2 \geq 0$ . Taking the limit for  $\epsilon \rightarrow 0$  shows that  $\ell(\nu) \leq \lambda + \mu$ .  $\square$

**4.3. Segre–Veronese manifolds.** By leveraging [Lemma 2.3](#) and [Theorem 4.4](#), minimizing geodesics on the Segre–Veronese manifold  $\mathcal{S}_\alpha^{\mathbf{k}}$  that connect two rank-1 tensors are readily obtained. Indeed, a minimizing geodesic connecting  $\mathcal{P}, Q \in \mathcal{S}_\alpha^{\mathbf{k}}$  is the pushforward of any geodesic whose length coincides with

$$\min_{p \in \otimes^{-1}(\mathcal{P}), q \in \otimes^{-1}(Q)} \text{dist}_{\mathcal{P}_\alpha^{\mathbf{k}}}(p, q).$$

[Corollary 4.6](#) then leads us naturally to the following terminology.

**DEFINITION 4.9 (Matched representations).** *Let  $\mathcal{P}, Q \in \mathcal{S}_\alpha^{\mathbf{k}}$ . We say that the representations  $p^* \in \otimes^{-1}(\mathcal{P})$  and  $q^* \in \otimes^{-1}(Q)$  are matched if*

$$(p^*, q^*) \in \arg \min_{p \in \otimes^{-1}(\mathcal{P}), q \in \otimes^{-1}(Q)} M(p, q),$$

where  $M$  is the distance from [Definition 4.1](#).

We are now ready to state and prove the main result about minimizing geodesics connecting two rank-1 tensors on the  $\alpha$ -warped Segre–Veronese manifold.

**THEOREM 4.10** (The logarithmic map of  $\mathcal{S}_\alpha^{\mathbf{k}}$ ). *Let  $\mathcal{P}, \mathcal{Q} \in \mathcal{S}_\alpha^{\mathbf{k}}$  be rank-1 tensors. If  $p = (\lambda, \mathbf{u}_1, \dots, \mathbf{u}_d) \in \otimes^{-1}(\mathcal{P})$  and  $q = (\mu, \mathbf{v}_1, \dots, \mathbf{v}_d) \in \otimes^{-1}(\mathcal{Q})$  are matched,  $\alpha$ -compatible representations, then*

$$\log_p \mathcal{Q} = (d_p \otimes)(\log_p q).$$

*Proof.* Combine [Corollary 4.6](#), [Definition 4.9](#), and [Theorem 4.4](#).  $\square$

The straightforward approach to determine matched representations of  $\mathcal{P}, \mathcal{Q} \in \mathcal{S}_\alpha^{\mathbf{k}}$  consists of choosing an arbitrary  $p^* \in \otimes^{-1}(\mathcal{P})$  and then computing all distances  $M(p^*, q)$  for all  $q \in \otimes^{-1}(\mathcal{Q})$  and selecting a minimum. By [Lemma 2.2](#), the possible  $q$  can be labeled by  $(\sigma_1, \dots, \sigma_d) \in \{-1, 1\}^d$  such that  $\sigma_1^{k_1} \dots \sigma_d^{k_d} = 1$ . Thus this strategy has a computational complexity of  $\mathcal{O}(2^d \dim \mathcal{S}_\alpha^{\mathbf{k}})$ , where  $\mathcal{O}(\dim \mathcal{S}_\alpha^{\mathbf{k}})$  is the asymptotic cost for computing one distance  $M(p^*, q)$ . We now explain how a matched representation can be constructed efficiently in  $\mathcal{O}(d \dim \mathcal{S}_\alpha^{\mathbf{k}})$  operations.

Let  $q_{\text{ref}} \in \otimes^{-1}(\mathcal{Q})$  be a reference preimage. We then observe that

$$M(p^*, q)^2 = M(p^*, q_{\text{ref}})^2 + \sum_{i=1}^d \frac{1 - \sigma_i}{2} \Delta_i.$$

with  $\Delta_i = k_i((\angle_i - \pi)^2 - \angle_i^2)$ , where  $\angle_i$  is the angle between the  $i$ th components of  $p^*$  and  $q_{\text{ref}}$ . Minimizing  $M(p^*, q)$  thus corresponds to maximizing  $\sum_{i=1}^d \sigma_i \Delta_i$  over  $\sigma_i \in \{-1, 1\}$ . An unconstrained optimum is

$$(4.4) \quad \sigma_i = \begin{cases} 1, & \text{if } \Delta_i \text{ is nonnegative,} \\ -1, & \text{otherwise.} \end{cases}$$

If this assignment also satisfies the constraint  $\sigma_1^{k_1} \dots \sigma_d^{k_d} = 1$ , so that  $q \in \otimes^{-1}(q_{\text{ref}})$ , then we are done. Otherwise, there is at least one smallest  $|\Delta_\ell|$  among the odd  $k_\ell$ 's. The sign of the corresponding  $\sigma_\ell$  should be flipped.

**PROPOSITION 4.11** (Matchmaking). *The algorithm described in the previous paragraph produces matched representations.*

*Proof.* A detailed proof is given in [Appendix A.3](#).  $\square$

The construction of the matchmaking algorithm suggests that determining an analogue of [Proposition 4.3](#) is more complicated for the Segre–Veronese manifold. Essentially, we have to consider the following problem: Given  $p^* \in \mathcal{P}_\alpha^{\mathbf{k}}$ , what is the set of  $q \in \mathcal{P}_\alpha^{\mathbf{k}}$  such that the corresponding matched representations  $q^* \in \mathcal{P}_\alpha^{\mathbf{k}}$  are  $\alpha$ -compatible with  $p^*$ , and when is this set the whole of  $\mathcal{P}_\alpha^{\mathbf{k}}$ ? By our calculations, this question can be reduced to a combinatorial optimization problem. As we were unable to produce a closed form of its solution, we present only the following general result.

**PROPOSITION 4.12.** *The Segre–Veronese manifold  $\mathcal{S}_\alpha^{\mathbf{k}}$  is geodesically connected if  $0 < \alpha < 1/\sqrt{k_1 + \dots + k_d}$  and is not geodesically connected if  $2/\sqrt{k_1 + \dots + k_d} \leq \alpha$ .*

*Proof.* The first statement is a corollary of [Lemma 2.2](#) and [Proposition 4.3](#).

To prove the second statement, assume  $\alpha \geq 2/\sqrt{k_1 + \dots + k_d}$  and pick  $p, q \in \mathcal{P}_\alpha^{\mathbf{k}}$  with angles  $\angle_1 = \dots = \angle_d = \frac{\pi}{2}$  between their components. These two representations are matched. However, using  $M(p, q)^2 = (k_1 + \dots + k_d) \frac{\pi^2}{4}$  in [Definition 4.1](#) shows that they are not  $\alpha$ -compatible.  $\square$

For  $1/\sqrt{k_1 + \dots + k_d} < \alpha < 2/\sqrt{k_1 + \dots + k_d}$ , geodesic connectedness is more complicated and depends also on the parity of the  $k_i$ 's. The full analysis is beyond the scope of this article.

**5. Sectional curvature.** Formulae for the sectional curvature of a manifold are useful in many situations, for example when approximating or compressing data that lives on said manifold [25,45,85], or to ensure uniqueness of the Fréchet mean [3,48,49], as required in the experiment from section 6. We compute these curvatures here for the  $\alpha$ -warped Segre–Veronese manifolds.

Consider first the  $\alpha$ -warped Segre manifold  $\mathcal{S}_\alpha = \mathcal{S}_\alpha^{(1,\dots,1)}$ . To compute its curvature, we recall the following general result about warped products.

PROPOSITION 5.1 (O’Neill [71, 7.42]). *For  $(a, b) \in \mathcal{M} \times_f \mathcal{N}$ , let  $\dot{\mathbf{x}}, \dot{\mathbf{y}}, \dot{\mathbf{z}} \in T_a\mathcal{M}$  and  $\dot{\mathbf{u}}, \dot{\mathbf{v}}, \dot{\mathbf{w}} \in T_b\mathcal{N}$  be tangent vectors, which naturally lift to  $T_{(a,b)}(\mathcal{M} \times_f \mathcal{N})$ . Let  $R_{\mathcal{M}}$  and  $R_{\mathcal{N}}$  be the Riemann tensors on  $\mathcal{M}$  and  $\mathcal{N}$ , respectively. Then, the Riemann tensor  $R$  on  $\mathcal{M} \times_f \mathcal{N}$  is described by:<sup>2</sup>*

1.  $R(\dot{\mathbf{x}}, \dot{\mathbf{y}})\dot{\mathbf{z}} = R_{\mathcal{M}}(\dot{\mathbf{x}}, \dot{\mathbf{y}})\dot{\mathbf{z}}$ ,
2.  $R(\dot{\mathbf{u}}, \dot{\mathbf{x}})\dot{\mathbf{y}} = -\frac{1}{f} \text{Hess}[f](\dot{\mathbf{x}}, \dot{\mathbf{y}})\dot{\mathbf{u}}$ ,
3.  $R(\dot{\mathbf{x}}, \dot{\mathbf{y}})\dot{\mathbf{u}} = 0$ ,
4.  $R(\dot{\mathbf{u}}, \dot{\mathbf{v}})\dot{\mathbf{x}} = 0$ ,
5.  $R(\dot{\mathbf{x}}, \dot{\mathbf{u}})\dot{\mathbf{v}} = -\frac{\langle \dot{\mathbf{u}}, \dot{\mathbf{v}} \rangle}{f} \nabla_{\dot{\mathbf{x}}}(\text{grad } f)$ ,
6.  $R(\dot{\mathbf{u}}, \dot{\mathbf{v}})\dot{\mathbf{w}} = R_{\mathcal{N}}(\dot{\mathbf{u}}, \dot{\mathbf{v}})\dot{\mathbf{w}} + \frac{\|\text{grad } f\|^2}{f^2} (\langle \dot{\mathbf{u}}, \dot{\mathbf{w}} \rangle \dot{\mathbf{v}} - \langle \dot{\mathbf{v}}, \dot{\mathbf{w}} \rangle \dot{\mathbf{u}})$ .

Herein,  $\langle \cdot, \cdot \rangle$  is the inner product on  $T_{(a,b)}(\mathcal{M} \times_f \mathcal{N})$ ,  $\text{grad } f$  is the Riemannian gradient of  $f$ ,  $\text{Hess}[f]$  is the Riemannian Hessian of  $f$ , and  $\nabla$  is the Levi–Civita connection.

For  $\mathcal{S}_\alpha$ , which locally looks like the warped product manifold  $\mathcal{P}_\alpha$ , these expressions simplify considerably. Applying Proposition 5.1 to  $\mathcal{N} = \mathbb{S}^{\mathbf{n},1} = \mathbb{S}^{n_1-1} \times \dots \times \mathbb{S}^{n_d-1}$  and  $\mathcal{M} = \mathbb{R}_{>0}$  while observing that  $\text{grad } f = \alpha$  and  $R_{\mathcal{M}} = 0$  yields the next result.

COROLLARY 5.2. *In the notation of Proposition 5.1, the Riemann tensor  $R$  of  $\mathcal{S}_\alpha$  at  $\lambda \mathbf{u}_1 \otimes \dots \otimes \mathbf{u}_d$  satisfies*

$$R(\dot{\mathbf{u}}, \dot{\mathbf{v}})\dot{\mathbf{w}} = R_{\mathbb{S}^{\mathbf{n},1}}(\dot{\mathbf{u}}, \dot{\mathbf{v}})\dot{\mathbf{w}} + \frac{1}{\lambda^2} (\langle \dot{\mathbf{u}}, \dot{\mathbf{w}} \rangle \dot{\mathbf{v}} - \langle \dot{\mathbf{v}}, \dot{\mathbf{w}} \rangle \dot{\mathbf{u}}),$$

and it is 0 in the remaining directions.

As sectional curvatures can be defined in terms of the Riemann tensor, we quickly find the next consequence of the last result.

COROLLARY 5.3. *For  $(\mathbf{u}_1, \dots, \mathbf{u}_d) \in \mathbb{S}^{\mathbf{n},1}$ , let the lifts of the tangent vectors  $\dot{\mathbf{u}}_i \in T_{\mathbf{u}_i}\mathbb{S}^{n_i-1}$  and  $\dot{\mathbf{v}}_j \in T_{\mathbf{u}_j}\mathbb{S}^{n_j-1}$  be orthonormal with respect to  $\langle \cdot, \cdot \rangle_{\mathcal{P}_\alpha}$ . The sectional curvature  $K$  of  $\mathcal{S}_\alpha$  at  $\lambda \mathbf{u}_1 \otimes \dots \otimes \mathbf{u}_d$  satisfies*

$$K(\dot{\mathbf{u}}_i, \dot{\mathbf{v}}_j) = \begin{cases} \frac{1-\alpha^2}{\alpha^2\lambda^2}, & \text{if } i = j, \\ -\frac{1}{\lambda^2}, & \text{otherwise,} \end{cases}$$

and  $K = 0$  in all remaining directions.

*Proof.* Recall that  $\langle \dot{\mathbf{u}}_i, \dot{\mathbf{v}}_j \rangle_{\mathcal{P}_\alpha} = \alpha^2 \lambda^2 \langle \dot{\mathbf{u}}_i, \dot{\mathbf{v}}_j \rangle_{\mathbb{S}^{\mathbf{n},1}}$ . We compute

$$\begin{aligned} K(\dot{\mathbf{u}}_i, \dot{\mathbf{v}}_j) &= \langle R(\dot{\mathbf{u}}_i, \dot{\mathbf{v}}_j)\dot{\mathbf{v}}_j, \dot{\mathbf{u}}_i \rangle_{\mathcal{P}_\alpha} \\ &= \langle R_{\mathbb{S}^{\mathbf{n},1}}(\dot{\mathbf{u}}_i, \dot{\mathbf{v}}_j)\dot{\mathbf{v}}_j, \dot{\mathbf{u}}_i \rangle_{\mathcal{P}_\alpha} + \frac{1}{\lambda^2} (\langle \dot{\mathbf{u}}_i, \dot{\mathbf{v}}_j \rangle_{\mathcal{P}_\alpha}^2 - \langle \dot{\mathbf{v}}_j, \dot{\mathbf{v}}_j \rangle_{\mathcal{P}_\alpha} \langle \dot{\mathbf{u}}_i, \dot{\mathbf{u}}_i \rangle_{\mathcal{P}_\alpha}) \\ &= \alpha^2 \lambda^2 \langle R_{\mathbb{S}^{\mathbf{n},1}}(\dot{\mathbf{u}}_i, \dot{\mathbf{v}}_j)\dot{\mathbf{v}}_j, \dot{\mathbf{u}}_i \rangle_{\mathbb{S}^{\mathbf{n},1}} - \frac{1}{\lambda^2} \end{aligned}$$

<sup>2</sup>Note that we use a definition of  $R$  that is consistent with [56] rather than [71]. The result is that some signs differ in our expressions from theirs.



$$\begin{aligned}
 &= \frac{\alpha^2 \lambda^2}{\alpha^4 \lambda^4} \langle R_{\mathbb{S}^{n,1}}(\alpha \lambda \dot{\mathbf{u}}_i, \alpha \lambda \dot{\mathbf{v}}_j) \alpha \lambda \dot{\mathbf{v}}_j, \alpha \lambda \dot{\mathbf{u}}_i \rangle_{\mathbb{S}^{n,1}} - \frac{1}{\lambda^2} \\
 &= \frac{1}{\alpha^2 \lambda^2} K_{\mathbb{S}^{n,1}}(\alpha \lambda \dot{\mathbf{u}}_i, \alpha \lambda \dot{\mathbf{v}}_j) - \frac{1}{\lambda^2} \\
 &= \frac{1}{\alpha^2 \lambda^2} \delta_{ij} - \frac{1}{\lambda^2}.
 \end{aligned}$$

In all other directions the sectional curvature is 0, because  $R = 0$  in these directions.  $\square$

The Segre–Veronese manifold  $\mathcal{S}_\alpha^{\mathbf{k}}$ ,  $\mathbf{k} = (k_1, \dots, k_d)$ , is a Riemannian submanifold of the Segre manifold  $\mathcal{S}_\alpha^{\mathbf{1}}$ , where  $\mathbf{1}$  is a vector of  $k_1 + \dots + k_d$  ones. If we look closely at the expression in [Proposition 3.1](#) for geodesics on  $\mathcal{S}_\alpha^{\mathbf{1}}$ , we see that starting out in a tangent direction to  $\mathcal{S}_\alpha^{\mathbf{k}} \subset \mathcal{S}_\alpha^{\mathbf{1}}$  produces a path wholly contained in  $\mathcal{S}_\alpha^{\mathbf{k}}$ . We have thus proved the following result.

**PROPOSITION 5.4.** *The Segre–Veronese manifold  $\mathcal{S}_\alpha^{\mathbf{k}}$  is a totally geodesic submanifold of the Segre manifold  $\mathcal{S}_\alpha^{\mathbf{1}}$ , and so its sectional curvature is described by restricting  $K$  in [Corollary 5.3](#) to the appropriate tangent subspace.*

**6. Numerical experiment.** The  $\alpha$ -warped Segre–Veronese manifold  $\mathcal{S}_\alpha^{\mathbf{k}}$  was implemented in Julia, including connecting and starting geodesics and the geodesic distance. Our implementation is available publicly [\[44\]](#).

As a numerical example illustration of the connecting geodesics in the  $\alpha$ -warped geometry of the Segre manifold, we recall the *consensus aggregation problem* from Chafamo, Shanmugam, and Tokcan [\[15\]](#): Given  $M$  approximate *tensor rank decompositions* of the same tensor  $\mathcal{A} \in \mathbb{R}^{n_1 \times \dots \times n_d}$ ,

$$\mathcal{A} \approx \mathcal{A}^{(m)} := \sum_{i=1}^r \mathcal{A}_i^{(m)} := \sum_{i=1}^r \mathbf{a}_{1i}^{(m)} \otimes \dots \otimes \mathbf{a}_{di}^{(m)}, \quad m = 1, \dots, M,$$

estimate the true decomposition of  $\mathcal{A}$ .

To solve the above problem, a consensus aggregation algorithm was proposed in [\[15\]](#) that takes elementwise medians of corresponding vectors  $\mathbf{a}_{ki}^{(m)}$ ,  $m = 1, \dots, M$ , of matching summands in the decomposition. While tensor rank decompositions usually have generically unique decompositions into a set of rank-1 tensors [\[5, 63, 82\]](#), to perform aggregation one needs to determine how these rank-1 tensors match up across multiple decompositions. For this reason, the rank-1 tensors are first matched using a ( $k$ -means) clustering algorithm in [\[15\]](#). This strategy can work well if the decomposition problem is well-conditioned [\[11\]](#), so that  $\mathcal{A}^{(m)}$  being close to  $\mathcal{A}$  will imply that the corresponding rank-1 tensors are close too. After matching up the rank-1 tensors, the results are aggregated in [\[15\]](#) by setting

$$\widehat{\mathbf{a}}_i^k = \text{median}(\mathbf{a}_{ki}^{(m)} : m = 1, \dots, M), \quad i = 1, \dots, r, \quad k = 1, \dots, d.$$

The median is taken elementwise. Note that it is possible for  $\widehat{\mathbf{a}}_i^k$  to have different values if different representatives are chosen. This is circumvented in [\[15\]](#) by aggregating positive data, for which there is a natural, positive, representative. The aggregated tensor decomposition is then

$$\mathcal{A} \approx \widehat{\mathcal{A}} := \sum_{i=1}^r \widehat{\mathbf{a}}_i^1 \otimes \dots \otimes \widehat{\mathbf{a}}_i^d.$$

The above is a simplified description of the essential ingredients of [\[15, Section 3\]](#).

From a geometric viewpoint, it is natural to estimate each rank-1 tensor with the Fréchet mean on the warped Segre manifold  $\mathcal{S}_\alpha$ . Recall that the Fréchet mean or Riemannian center of mass of points  $x_1, \dots, x_k$  on a Riemannian manifold  $\mathcal{M}$  is

$$\text{mean}_{\mathcal{M}}(x_1, \dots, x_k) = \arg \min_{p \in \mathcal{M}} \sum_{i=1}^n \text{dist}_{\mathcal{M}}(p, p_i)^2.$$

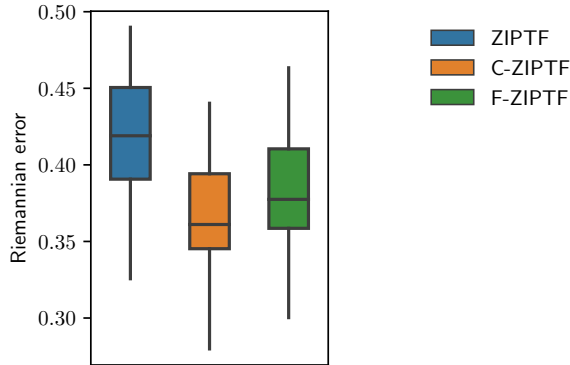


FIGURE 6.1. We recreate the setup from [15, Section 4.1] and compare the Riemannian distance between the approximate decompositions and the ground truth.

Its uniqueness has been investigated among others in [3, 48, 49]. For manifolds with negative sectional curvatures, the Fréchet mean is unique and the above defines a valid function. Hence, we propose to estimate  $\mathcal{A}$  instead as

$$\mathcal{A} \approx \tilde{\mathcal{A}} := \sum_{i=1}^r \tilde{\mathcal{A}}_i, \quad \text{where } \tilde{\mathcal{A}}_i = \text{mean}_{\mathcal{S}_\alpha}(\mathcal{A}_i^{(1)}, \dots, \mathcal{A}_i^{(M)}), \quad i = 1, \dots, r.$$

To guarantee that all points are comparable so that the Fréchet mean is well defined, we choose  $\alpha = 1/\sqrt{k_1 + \dots + k_d} - \sqrt{\epsilon}$  where  $\epsilon$  is the machine precision of double-precision floating-point numbers. Proposition 4.12 then guarantees all points are comparable.

We reproduce the experiment from [15, Section 4.1], using the authors' code with the same parameter values and initialization seed. Figure 6.1 compares our estimate to their estimate and to the baseline of doing no consensus aggregation. The baseline, ZIPTF, consists of just doing one zero-inflated Poisson tensor factorization as described in [15, Section 3.2]. C-ZIPTF is the consensus aggregation of 20 ZIPTF's by Chafamo, Shanmugam, and Tokcan's proposed method of medians. F-ZIPTF is similarly the consensus aggregation of 20 ZIPTF's by our proposed method of Fréchet means. The Fréchet mean is approximated by successive geodesic interpolation, see for example [16–18, 21]. We conclude that the accuracy of both consensus variants is better than the baseline. There does not appear to be a meaningful difference between C-ZIPTF and F-ZIPTF. This nevertheless validates the correctness and utility of connecting geodesics for the  $\alpha$ -warped Segre manifold.

The Julia source code for the experiments is available publicly [43].

## Appendix A. Proof of the technical lemmata.

**A.1. Proof of Lemma 2.2.** Each  $\iota_\sigma$  is an isometry because  $\mathcal{P}_\alpha^{\mathbf{k}}$  is a product manifold where  $\iota_\sigma$  acts only on the spheres and the maps Id and  $-\text{Id}$  are basic isometries of the sphere with the standard Euclidean inner product, and hence also with any scaled inner product.

Normality, i.e.,  $\otimes(p) = \otimes(q)$  implies there exists a  $\sigma$  such that  $q = \iota_\sigma(p)$  [71, Appendix A], follows from the multilinearity of the tensor product  $\otimes$  [34, Chapter 1].

By the same arguments as [6, Section 4.1],  $\otimes$  is a smooth covering map. Hence  $\dim \mathcal{P}_\alpha^{\mathbf{k}} = \dim \mathcal{S}_\alpha^{\mathbf{k}}$  and the differential  $d\otimes : T\mathcal{P}_\alpha^{\mathbf{k}} \rightarrow T\mathcal{S}_\alpha^{\mathbf{k}}$  is everywhere left-invertible.

The key part is showing that  $\otimes : \mathcal{P}_\alpha^{\mathbf{k}} \rightarrow \mathcal{S}_\alpha^{\mathbf{k}}$  is Riemannian, i.e., the metric of  $\mathcal{S}_\alpha^{\mathbf{k}}$  is the pushforward of the one of  $\mathcal{P}_\alpha^{\mathbf{k}}$ , which is a straightforward computation. Let  $\dot{\mathbf{u}}_i \in T_{\mathbf{u}_i} \mathbb{S}^{n_i-1} = \mathbf{u}_i^\perp$  and  $\dot{\lambda} \in \mathbb{R}$  be arbitrary. By differentiating  $\otimes : \mathcal{P}_\alpha^{\mathbf{k}} \rightarrow \mathcal{S}_\alpha^{\mathbf{k}}$ , we get

$$\begin{aligned} & (d(\lambda, \mathbf{u}_1, \dots, \mathbf{u}_d) \otimes (\dot{\lambda}, \dot{\mathbf{u}}_1, \dots, \dot{\mathbf{u}}_d)) \\ &= \dot{\lambda} \mathcal{U} + \lambda (\dot{\nu}_{k_1}(\dot{\mathbf{u}}_1) \otimes \mathbf{u}_2^{\otimes k_2} \otimes \dots \otimes \mathbf{u}_d^{\otimes k_d}) + \dots + \lambda (\mathbf{u}_1^{\otimes k_1} \otimes \dots \otimes \mathbf{u}_{d-1}^{\otimes k_{d-1}} \otimes \dot{\nu}_{k_d}(\dot{\mathbf{u}}_d)), \end{aligned}$$

where  $\mathcal{U}$  and  $\nu_k(\mathbf{u})$  are as in (3.7) and (3.8). The  $\alpha$ -warped metric on  $\mathcal{S}_\alpha^{\mathbf{k}}$  satisfies

$$\varsigma_{\lambda \mathcal{U}}^\alpha (d \otimes (\dot{x}, \dot{\mathbf{u}}_1, \dots, \dot{\mathbf{u}}_d), d \otimes (\dot{y}, \dot{\mathbf{v}}_1, \dots, \dot{\mathbf{v}}_d)) = \dot{x} \dot{y} + (\alpha \lambda)^2 \langle \dot{\mathcal{U}}, \dot{\mathcal{V}} \rangle,$$

having dropped the subscript  $(\lambda, \mathbf{u}_1, \dots, \mathbf{u}_d)$  of the differential and where

$$\begin{aligned} \dot{\mathcal{U}} &= (\dot{\nu}_{k_1}(\dot{\mathbf{u}}_1) \otimes \mathbf{u}_2^{\otimes k_2} \otimes \dots \otimes \mathbf{u}_d^{\otimes k_d}) + \dots + (\mathbf{u}_1^{\otimes k_1} \otimes \dots \otimes \mathbf{u}_{d-1}^{\otimes k_{d-1}} \otimes \dot{\nu}_{k_d}(\dot{\mathbf{u}}_d)), \\ \dot{\mathcal{V}} &= (\dot{\nu}_{k_1}(\dot{\mathbf{v}}_1) \otimes \mathbf{u}_2^{\otimes k_2} \otimes \dots \otimes \mathbf{u}_d^{\otimes k_d}) + \dots + (\mathbf{u}_1^{\otimes k_1} \otimes \dots \otimes \mathbf{u}_{d-1}^{\otimes k_{d-1}} \otimes \dot{\nu}_{k_d}(\dot{\mathbf{v}}_d)). \end{aligned}$$

Recall from [37] that the Euclidean inner product between rank-1 tensors satisfies  $\langle \mathbf{u}_1 \otimes \dots \otimes \mathbf{u}_d, \mathbf{v}_1 \otimes \dots \otimes \mathbf{v}_d \rangle = \prod_{i=1}^d \langle \mathbf{u}_i, \mathbf{v}_i \rangle$ . Hence, rank-1 tensors are orthogonal to one another if they are orthogonal in at least one factor. We compute that  $\langle \nu_{k_i}(\dot{\mathbf{u}}_i), \mathbf{u}_i^{\otimes k_i} \rangle = 0$ , while  $\langle \nu_{k_i}(\dot{\mathbf{u}}_i), \nu_{k_i}(\dot{\mathbf{v}}_i) \rangle = k_i \langle \dot{\mathbf{u}}_i, \dot{\mathbf{v}}_i \rangle$  if  $\dot{\mathbf{u}}_i, \dot{\mathbf{v}}_i \in T_{\mathbf{u}_i} \mathbb{S}^n$ . As a consequence, we can observe that the cross terms in  $\langle \dot{\mathcal{U}}, \dot{\mathcal{V}} \rangle$  vanish and we are left with

$$\langle \dot{\mathcal{U}}, \dot{\mathcal{V}} \rangle = \sum_{i=1}^d \langle \dot{\nu}_{k_i}(\dot{\mathbf{u}}_i), \dot{\nu}_{k_i}(\dot{\mathbf{v}}_i) \rangle = \sum_{i=1}^d k_i \langle \dot{\mathbf{u}}_i, \dot{\mathbf{v}}_i \rangle.$$

This shows that  $\varsigma_{\lambda \mathcal{U}}$  is the pushforward of  $g_{\lambda, \mathbf{u}_1, \dots, \mathbf{u}_d}$  under  $\otimes$ , concluding the proof.

**A.2. Proof of Lemma 2.3.** Every smooth curve on  $\mathcal{N}$  has such a unique smooth lift through a normal covering by [71, Lemma A.9]. Moreover, as  $\phi$  is a local isometry that restricts to an isometry on evenly covered neighborhoods, the length of  $\gamma$  and its unique lift  $\tilde{\gamma}$  in  $\mathcal{M}$  coincide. Indeed, if we partition the lift  $\tilde{\gamma}$  into the curve segments  $\tilde{\gamma}_i$  such that  $\tilde{\gamma}_i \subset \mathcal{M}_i \subset \mathcal{M}$  with  $\phi|_{\mathcal{M}_i} : \mathcal{M}_i \rightarrow \mathcal{N}_i$  an isometry (such a partition exists and is used to prove the existence of a unique lift in [71, Lemma A.9]), then

$$\ell(\tilde{\gamma}) = \sum_{i=1}^k \ell(\tilde{\gamma}_i) = \sum_{i=1}^k \ell(\phi(\tilde{\gamma}_i)) = \ell(\gamma).$$

This concludes the first part of the proof.

If there were a strictly shorter smooth curve  $\tilde{\gamma}' \subset \mathcal{M}$  connecting the endpoints of the lift  $\tilde{\gamma}$ , then by the same partitioning argument  $\phi \circ \tilde{\gamma}' \subset \mathcal{N}$  would be a shorter piecewise smooth curve ( $\phi$  is a local embedding) than  $\gamma$ , contradicting its minimality. This proves the second part.

**A.3. Proof of Proposition 4.11.** We want to maximize  $f = \sum_{i=1}^d \sigma_i \Delta_i$  over  $\sigma_i \in \{-1, 1\}$  with the constraint that  $\sigma_1^{k_1} \dots \sigma_d^{k_d} = 1$ .

We can assume without loss of generality that all  $k_i$ 's are odd. Indeed, even  $k_i$  do not impact the constraint, so we can choose the corresponding sign so that  $|\Delta_i| = \sigma_i \Delta_i$ , which is clearly optimal, also without constraint, because of the bilinear structure of  $f$ . The matching algorithm chooses these signs precisely in this way.

We can further assume without loss of generality that all  $\Delta_i$  are nonzero, for otherwise we could take the unconstrained optimum (4.4) and simply swap the sign of a  $\sigma_j$  for which  $\Delta_j = 0$  to obtain a feasible solution that is also globally optimal, which is what the matching algorithm does.

Let  $(\varsigma_1, \dots, \varsigma_d)$  be a constrained optimizer of  $f$  that differs in the least number of indices from the unconstrained optimizer  $(\sigma_1, \dots, \sigma_d)$  from (4.4). Denote the number of different indices by  $p = \#\{i \in \{1, \dots, d\} \mid \sigma_i \neq \varsigma_i\}$ . Then, there are three cases:

$p = 0$ . The unconstrained optimum given by (4.4) and chosen by the algorithm satisfies the constraint.

- $p = 1$ . If  $f_0$  denotes the value of  $f$  for the unconstrained optimum, such a constrained optimum has value  $f_0 - 2|\Delta_i|$ . Hence,  $i$  must correspond to the minimal  $|\Delta_i|$ , which the matching algorithm indeed selects by construction.
- $p \geq 2$ . Let  $i \neq j$  be any two indices for which  $\varsigma_i \neq \sigma_i$  and  $\varsigma_j \neq \sigma_j$ . By changing the signs of  $\varsigma_i$  and  $\varsigma_j$  to match those of  $\sigma_i$  and  $\sigma_j$ , respectively, this increases the objective by  $2|\Delta_i| + 2|\Delta_j|$ . Since  $|\Delta_i|, |\Delta_j| > 0$ , this modified, feasible constrained point with  $p - 2$  different indices has a strictly higher objective value than  $(\varsigma_1, \dots, \varsigma_d)$ , which was supposed to be the constrained minimizer with minimal  $p$ . This is a contradiction, so this case cannot occur.

This concludes the proof.

#### REFERENCES

- [1] P.-A. ABSIL, R. MAHONY, AND R. SEPULCHRE, *Optimization Algorithms on Matrix Manifolds*, Princeton University Press, 2008.
- [2] P.-A. ABSIL AND J. MALICK, *Projection-like retractions on matrix manifolds*, SIAM J. Optim., 22 (2012), pp. 135–158.
- [3] B. AFSARI, *Riemannian  $L^p$  center of mass: Existence, uniqueness, and convexity*, Proc. Amer. Math. Soc., 139 (2011), pp. 655–655.
- [4] A. ANANDKUMAR, R. GE, D. HSU, S. M. KAKADE, AND M. TELGARSKY, *Tensor decompositions for learning latent variable models*, J. Mach. Learn. Res., 15 (2014), pp. 2773–2832.
- [5] E. BALLICO, *Joins, secant varieties and their associated Grassmannians*, Mathematics, 12 (2024), p. 1274.
- [6] C. BELTRÁN, P. BREIDING, AND N. VANNIEUWENHOVEN, *Pencil-based algorithms for tensor rank decomposition are not stable*, SIAM J. Matrix Anal. Appl., 40 (2019), pp. 739–773.
- [7] A. BERNARDI, E. CARLINI, M. V. CATALISANO, A. GIMIGLIANO, AND A. ONETO, *The hitchhiker guide to: Secant varieties and tensor decomposition*, Mathematics, 6 (2018).
- [8] X. BI, X. TANG, Y. YUAN, Y. ZHANG, AND A. QU, *Tensors in statistics*, Ann. Rev. Stat. Appl., 8 (2021), pp. 345–368.
- [9] N. BOUMAL, *An Introduction to Optimization on Smooth Manifolds*, Cambridge University Press, Mar. 2023.
- [10] N. BOUMAL AND P.-A. ABSIL, *A discrete regression method on manifolds and its application to data on  $so(n)$* , IFAC Proceedings Volumes, 44 (2011), pp. 2284–2289.
- [11] P. BREIDING AND N. VANNIEUWENHOVEN, *The condition number of join decompositions*, SIAM J. Matrix Anal. Appl., 39 (2018), pp. 287–309.
- [12] ———, *A Riemannian trust region method for the canonical tensor rank approximation problem*, SIAM J. Optim., 28 (2018), pp. 2435–2465.
- [13] D. BURAGO, Y. BURAGO, AND S. IVANOV, *A Course in Metric Geometry*, vol. 33 of Graduate Series in Mathematics, American Mathematical Society, Providence, Rhode Island, 2001.
- [14] B. CARREL, M. J. GANDER, AND B. VANDEREYCKEN, *Low-rank parareal: a low-rank parallel-in-time integrator*, BIT, 63 (2023).
- [15] D. CHAFAMO, V. SHANMUGAM, AND N. TOKCAN, *Robust Bayesian tensor factorization with zero-inflated Poisson model and consensus aggregation*, arXiv:2308.08060v1, (2023).
- [16] R. CHAKRABORTY AND B. C. VEMURI, *Recursive Fréchet mean computation on the Grassmannian and its applications to computer vision*, in 2015 IEEE International Conference on Computer Vision (ICCV), 2015, pp. 4229–4237.
- [17] ———, *Statistics on the Stiefel manifold: Theory and applications*, Ann. Stat., 47 (2019), pp. 415–438.
- [18] ———, *Efficient recursive estimation of the Riemannian barycenter on the hypersphere and the special orthogonal group with applications*, in Riemannian Geometric Statistics in Medical Image Analysis, X. Pennec, S. Sommer, and T. Fletcher, eds., Academic Press, 2020, pp. 273–297.
- [19] A. CHAROUS AND P. F. J. LERMUSIAUX, *Stable rank-adaptive dynamically orthogonal Runge–Kutta schemes*, SIAM J. Sci. Comput., 46 (2024), pp. A529–A560.
- [20] C.-H. CHEN, *Warped products of metric spaces of curvature bounded from above*, Trans. Amer. Math. Soc., 351 (1999), pp. 4727–4740.
- [21] G. CHENG, J. HO, H. SALEHIAN, AND B. C. VEMURI, *Recursive Computation of the Fréchet Mean on Non-positively Curved Riemannian Manifolds with Applications*, Springer International Publishing, Cham, 2016, pp. 21–43.
- [22] P. COMON, G. H. GOLUB, L.-H. LIM, AND B. MOURRAIN, *Symmetric tensors and symmetric tensor rank*, SIAM J. Matrix Anal. Appl., 30 (2008), pp. 1254–1279.
- [23] P. E. CROUCH AND R. GROSSMAN, *Numerical integration of ordinary differential equations on manifolds*, J. Nonlinear Sci., 3 (1993), pp. 1–33.
- [24] L. DE LATHAUWER, B. DE MOOR, AND J. VANDEWALLE, *A multilinear singular value decom-*

- position, *SIAM J. Matrix Anal. Appl.*, 21 (2000), pp. 1253–1278.
- [25] W. DIEPEVEEN, J. CHEW, AND D. NEEDELL, *Curvature corrected tangent space-based approximation of manifold-valued data*, 2023.
- [26] A. EIBEN AND J. SMITH, *Introduction to Evolutionary Computing*, Springer, 2015.
- [27] F. FEPPON AND P. F. J. LERMUSIAUX, *A geometric approach to dynamical model order reduction*, *SIAM J. Matrix Anal. Appl.*, 39 (2018), pp. 510–538.
- [28] P. FLETCHER, C. LU, S. PIZER, AND S. JOSHI, *Principal geodesic analysis for the study of nonlinear statistics of shape*, *IEEE Trans. Med. Imaging*, 23 (2004), pp. 995–1005.
- [29] P. T. FLETCHER AND S. JOSHI, *Riemannian geometry for the statistical analysis of diffusion tensor data*, *Signal Process.*, 87 (2007), pp. 250–262.
- [30] T. P. FLETCHER, *Geodesic regression and the theory of least squares on Riemannian manifolds*, *Int. J. Comput. Vision*, 105 (2012), pp. 171–185.
- [31] ———, *Statistics on Manifolds*, Elsevier, 2020, pp. 39–74.
- [32] M. FRÉCHET, *Les éléments aléatoires de nature quelconque dans un espace distancié.*, *Ann. Inst. Fourier (Grenoble)*, 10 (1948), pp. 215–310.
- [33] P.-Y. GOUSENBOURGER, E. MASSART, AND P.-A. ABSIL, *Data fitting on manifolds with composite bézier-like curves and blended cubic splines*, *J. Math. Imaging Vision*, 61 (2018), pp. 645–671.
- [34] W. GREUB, *Multilinear Algebra*, Springer-Verlag, 2 ed., 1978.
- [35] P. GROHS, *Quasi-interpolation in Riemannian manifolds*, *IMA J. Numer. Anal.*, 33 (2012), pp. 849–874.
- [36] P. GROHS, M. SPRECHER, AND T. YU, *Scattered manifold-valued data approximation*, *Numer. Math.*, 135 (2016), pp. 987–1010.
- [37] W. HACKBUSCH, *Tensor Spaces and Numerical Tensor Calculus*, no. 42 in Springer Series in Computational Mathematics, Springer-Verlag, 2 ed., 2019.
- [38] E. HAIER, G. WANNER, AND C. LUBICH, *Geometric Numerical Integration*, Springer-Verlag, 2 ed., 2006.
- [39] E. HAIRER, *Geometric integration of ordinary differential equations on manifolds*, *BIT*, 41 (2001), pp. 996–1007.
- [40] U. HELMKE AND J. B. MOORE, *Optimization and Dynamical Systems*, Springer, 1994.
- [41] J. HINKLE, P. T. FLETCHER, AND S. JOSHI, *Intrinsic polynomials for regression on Riemannian manifolds*, *J. Math. Imaging Vision*, 50 (2014), pp. 32–52.
- [42] M. HOCHBRUCK, M. NEHER, AND S. SCHRAMMER, *Dynamical low-rank integrators for second-order matrix differential equations*, *BIT*, 63 (2023).
- [43] S. JACOBSSON. <https://gitlab.kuleuven.be/numa/public/alpha-warped-experiments>.
- [44] ———, *ManiFactor.jl: Approximating maps into manifolds*. <https://gitlab.kuleuven.be/numa/software/ManiFactor>, 2024.
- [45] S. JACOBSSON, R. VANDEBRIL, J. VAN DER VEKEN, AND N. VANNIEUWENHOVEN, *Approximating maps into manifolds with lower curvature bounds*, arXiv:2403.16785v1, (2024).
- [46] J. JAKUBIAK, F. SILVA LEITE, AND R. C. RODRIGUES, *A two-step algorithm of smooth spline generation on Riemannian manifolds*, *J. Comput. Appl. Math.*, 194 (2006), pp. 177–191.
- [47] B. JEURIS, R. VANDEBRIL, AND B. VANDEREYCKEN, *A survey and comparison of contemporary algorithms for computing the matrix geometric mean*, *Electron. Trans. Numer. Anal.*, 39 (2012), pp. 379–402.
- [48] H. KARCHER, *Riemannian center of mass and mollifier smoothing*, *Commun. Pure Appl. Math.*, 30 (1977), pp. 509–541.
- [49] W. S. KENDALL, *Probability, convexity, and harmonic maps with small image I: Uniqueness and fine existence*, *Proc. London Math. Soc.*, s3-61 (1990), pp. 371–406.
- [50] R. KHOUJA, H. KHALIL, AND B. MOURRAIN, *Riemannian Newton optimization methods for the symmetric tensor approximation problem*, *Linear Algebra Appl.*, 637 (2022), pp. 175–211.
- [51] O. KOCH AND C. LUBICH, *Dynamical low-rank approximation*, *SIAM J. Matrix Anal. Appl.*, 29 (2007), pp. 434–454.
- [52] ———, *Dynamical tensor approximation*, *SIAM J. Matrix Anal. Appl.*, 31 (2010), pp. 2360–2375.
- [53] T. G. KOLDA AND B. W. BADER, *Tensor decompositions and applications*, *SIAM Rev.*, 51 (2009), pp. 455–500.
- [54] D. KRESSNER, M. STEINLECHNER, AND B. VANDEREYCKEN, *Low-rank tensor completion by Riemannian optimization*, *BIT*, 54 (2014), pp. 447–468.
- [55] J. M. LANDSBERG, *Tensors: Geometry and Applications*, vol. 128 of Graduate Studies in Mathematics, AMS, Providence, Rhode Island, 2012.
- [56] J. M. LEE, *Riemannian Manifolds: Introduction to Curvature*, Springer Verlag, 1997.
- [57] D. LEWIS AND P. J. OLVER, *Geometric integration algorithms on homogeneous manifolds*, *Found. Comput. Math.*, 2 (2002), pp. 363–392.
- [58] L.-H. LIM, *Tensors in computations*, *Acta Numerica*, 30 (2021), pp. 555–764.
- [59] S. LOHIT AND P. TURAGA, *Learning invariant Riemannian geometric representations using deep nets*, in 2017 IEEE International Conference on Computer Vision Workshops (ICCVW), IEEE, Oct. 2017.

- [60] C. LUBICH, I. V. OSELEDETS, AND B. VANDEREYCKEN, *Time integration of tensor trains*, SIAM J. Numer. Anal., 53 (2015), pp. 917–941.
- [61] C. LUBICH, T. ROHWEDDER, R. SCHNEIDER, AND B. VANDEREYCKEN, *Dynamical approximation by hierarchical Tucker and tensor-train tensors*, SIAM J. Matrix Anal. Appl., 34 (2013), pp. 470–494.
- [62] L. MACHADO AND F. SILVA LEITE, *Fitting smooth paths on Riemannian manifolds*, Int. J. Appl. Math. Stat., 4 (2006), pp. 25–53.
- [63] A. MASSARENTI AND M. MELLA, *Bronowski’s conjecture and the identifiability of projective varieties*, Duke Math. J., (2024). accepted.
- [64] E. M. MASSART, J. M. HENDRICKX, AND P.-A. ABSIL, *Matrix geometric means based on shuffled inductive sequences*, Linear Algebra Appl., 542 (2018), pp. 334–359.
- [65] M. MØRUP, *Applications of tensor (multiway array) factorizations and decompositions in data mining*, Wiley Interdisciplinary Reviews: Data Mining and Knowledge Discovery, 1 (2011), pp. 24–40.
- [66] H. MUNTHE-KAAS, *Runge-kutta methods on lie groups*, BIT, 38 (1998), pp. 92–111.
- [67] H. MUNTHE-KAAS AND A. ZANNA, *Numerical Integration of Differential Equations on Homogeneous Manifolds*, Springer Berlin Heidelberg, 1997, pp. 305–315.
- [68] A. MUSOLAS, E. MASSART, J. M. HENDRICKX, P.-A. ABSIL, AND Y. MARZOUK, *Low-rank multi-parametric covariance identification*, BIT, 62 (2021), pp. 221–249.
- [69] E. NAVA-YAZDANI AND K. POLTHIER, *De Casteljau’s algorithm on manifolds*, Comput. Aided Geom. Des., 30 (2013), pp. 722–732.
- [70] L. NOAKES, G. HEINZINGER, AND B. PADEN, *Cubic splines on curved spaces*, IMA J. Math. Control Inf., 6 (1989), pp. 465–473.
- [71] B. O’NEILL, *Semi-Riemannian Geometry With Applications to Relativity*, Academic Press, July 1983.
- [72] E. E. PAPALEXAKIS, C. FALOUTSOS, AND N. D. SIDIROPOULOS, *Tensors for data mining and data fusion: Models, applications, and scalable algorithms*, ACM Trans. Intell. Syst. Technol., 8 (2016), pp. 1–44.
- [73] X. PENNEC, *Intrinsic statistics on Riemannian manifolds: Basic tools for geometric measurements*, J. Math. Imaging Vision, 25 (2006), pp. 127–154.
- [74] X. PENNEC, P. FILLARD, AND N. AYACHE, *A Riemannian framework for tensor computing*, Int. J. Comput. Vision, 66 (2006), pp. 41–66.
- [75] T. POPIEL AND L. NOAKES, *Bézier curves and  $C^2$  interpolation in Riemannian manifolds*, J. Approx. Theory, 148 (2007), pp. 111–127.
- [76] C. SAMIR AND I. ADOUANI,  *$C^1$  interpolating Bézier path on Riemannian manifolds, with applications to 3D shape space*, Appl. Math. Comput., 348 (2019), pp. 371–384.
- [77] N. SHARON, R. S. COHEN, AND H. WENDLAND, *On multiscale quasi-interpolation of scattered scalar- and manifold-valued functions*, SIAM J. Sci. Comput., 45 (2023), p. A2458–A2482.
- [78] N. D. SIDIROPOULOS, L. DE LATHAUWER, X. FU, K. HUANG, E. E. PAPALEXAKIS, AND C. FALOUTSOS, *Tensor decomposition for signal processing and machine learning*, IEEE Trans. Signal Process., 65 (2017), pp. 3551–3582.
- [79] S. SOMMER, F. LAUZE, AND M. NIELSEN, *Optimization over geodesics for exact principal geodesic analysis*, Adv. Comput. Math., 40 (2013), pp. 283–313.
- [80] L. SWIJSEN, *Tensor Decompositions and Riemannian Optimization: Applications of the Geometry of the Segre Manifold*, PhD thesis, KU Leuven, 2022.
- [81] L. SWIJSEN, J. VAN DER VEKEN, AND N. VANNIEUWENHOVEN, *Tensor completion using geodesics on Segre manifolds*, Numer. Linear Algebra Appl., 29 (2022).
- [82] A. TAVEIRA BLOMENHOFER AND A. CASAROTTI, *Nondefectivity of invariant secant varieties*, arXiv:2312.12335v2, (2024).
- [83] A. USCHMAJEW AND B. VANDEREYCKEN, *The geometry of algorithms using hierarchical tensors*, Linear Algebra Appl., 439 (2013), pp. 133–166.
- [84] R. ZIMMERMANN, *Hermite interpolation and data processing errors on Riemannian matrix manifolds*, SIAM J. Sci. Comput., 42 (2020), p. A2593–A2619.
- [85] ———, *Hermite interpolation and data processing errors on Riemannian matrix manifolds*, SIAM J. Sci. Comput., 42 (2020), pp. A2593–A2619.
- [86] ———, *Manifold interpolation*, De Gruyter, Oct. 2021, ch. 7, pp. 229–274.
- [87] R. ZIMMERMANN AND R. BERGMANN, *Multivariate Hermite interpolation on Riemannian manifolds*, SIAM J. Sci. Comput., 46 (2024), p. A1276–A1297.
- [88] R. ZIMMERMANN AND K. HÜPER, *Computing the Riemannian logarithm on the Stiefel manifold: Metrics, methods, and performance*, SIAM J. Matrix Anal. Appl., 43 (2022), pp. 953–980.